Published in final edited form as:
Chem Res Toxicol. 2011 July 18; 24(7): 1048–1061. doi:10.1021/tx200055c.

Identification and Characterization of 2′-Deoxyadenosine Adducts formed by Isoprene Monoepoxides *In Vitro*

Petra Begemann[†,⊥], **Gunnar Boysen**[†,‡,⊤], **Nadia I. Georgieva**[†,⊤], **Ramiah Sangaiah**[†], **Karl M. Koshlap**[§], **Hasan Koc**[†,┼], **Daping Zhang**[‖], **Bernard T. Golding**[‖], **Avram Gold**[†], and **James A. Swenberg**[†,‡,*]

Petra Begemann: pbegemann@environcorp.com; Gunnar Boysen: GBoysen@uams.edu; Nadia I. Georgieva: NIGeorgieva@uams.edu; Ramiah Sangaiah: rsangaiah@sophia.sph.unc.edu; Karl M. Koshlap: koshlap@email.unc.edu; Hasan Koc: huk12@psu.edu; Daping Zhang: daping.zhang@ncl.ac.uk; Bernard T. Golding: B.T.Golding@newcastle.ac.uk; Avram Gold: golda@email.unc.edu; James A. Swenberg: jswenber@email.unc.edu

[†] Department of Environmental Sciences and Engineering, The University of North Carolina at Chapel Hill, North Carolina 27599-7431

[‡] Center of Environmental Health and Susceptibility, The University of North Carolina at Chapel Hill, North Carolina 27599-7431

[§] School of Pharmacy, The University of North Carolina at Chapel Hill, Chapel Hill, North Carolina 27599-7360

[‖] School of Chemistry, Bedson Building, Newcastle University, Newcastle upon Tyne, NE1 7RU U.K

Abstract

Isoprene, the 2-methyl analog of 1,3-butadiene, is ubiquitous in the environment, with major contributions to total isoprene emissions stemming from natural processes despite the compound being a bulk industrial chemical. Additionally, isoprene is a combustion product and a major component in cigarette smoke. Isoprene has been classified as *possibly carcinogenic to humans (group 2B)* by IARC and as *reasonably anticipated to be a human carcinogen* by the National Toxicology Program. Isoprene, like butadiene, requires metabolic activation to reactive epoxides to exhibit its carcinogenic properties. The mode of action has been postulated to be that of a genotoxic carcinogen, with formation of promutagenic DNA adducts being essential for mutagenesis and carcinogenesis. In rodents, isoprene-induced tumors show unique point mutations (A→T transversions) in the K-*ras* protooncogene at codon 61. Therefore, we investigated adducts formed after reaction of 2′-deoxyadenosine (dAdo1) with the two monoepoxides of isoprene, 2-ethenyl-2-methyloxirane (IP-1,2-O) and propen-2-yloxirane (IP-3,4-O), under physiological conditions. The formation of N1–2′-deoxyinosine (N1-dIno) due to deamination of N1-dAdo adducts was of particular interest, since N1-dIno adducts are suspected to have high mutagenic

[1]**Abbreviations**: dAdo, 2′-deoxyadenosine; dIno, 2′-deoxyinosine; dR, deoxyribose; ESI-MS, positive ion electrospray mass spectrometry; IP-1,2-O, isoprene-1,2-oxide (2-ethenyl-2-methyloxirane); IP-3,4-O, isoprene-3,4-oxide (propen-2-yloxirane); $IPO_{commercial}$, commercially available 95 % isoprene-1,2-oxide with 5 % isoprene-3,4-oxide; MS/MS, tandem mass spectrometry.

[*]To whom correspondence should be addressed. Email: jswenber@email.unc.edu.
[⊥]Current Address: ENVIRON International Corporation, Health Sciences, 4350 North Fairfax Drive, Arlington, Virginia 22203
[⊤]Current Address: University of Arkansas for Medical Sciences, Department of Environmental and Occupational Health, Little Rock, Arkansas 72205
[┼]Current Address: Penn State University, Department of Biochemistry and Molecular Biology, University Park, Pennsylvania 16802

Supporting Information Available.
Table of accurate mass measurements of purified adducts; Schemes of Fragmentation of IP-1,2-O- and IP-3,4-O-derived N6-dAde adducts; MS/MS spectra of N^6-dAdo and N1-dIno adducts; complete 2D NMR spectra; HPLC/DAD analyses of *S*-IP-1,2-O with dAdo, *S*-IP-3,4-O with dAdo, IP-3,4-O with dIno, and *S*-IP-3,4-O with dIno. This material is available free of charge via the Internet at http://pubs.acs.org.

potential based on *in vitro* experiments. Major stable adducts were identified by HPLC, UV-Spectrometry and LC-MS/MS and characterized by ^{1}H and ^{1}H,^{13}C HSQC and NMR experiments. Adducts of IP-1,2-O that were fully identified are: *R*,*S*-C1-N^6-dAdo, *R*-C2-N^6-dAdo, and *S*-C2-N^6-dAdo; adducts of IP-3,4-O are: *S*-C3-N^6-dAdo, *R*-C3-N^6-dAdo, *R*,*S*-C4-N^6-dAdo, *S*-C4-N1-dIno, *R*-C4-N1-dIno, *R*-C3-N1-dIno, *S*-C3-N1-dIno, and C3-N7-Ade. Both monoepoxides formed adducts on the external and internal oxirane carbons. This is the first study to describe adducts of isoprene monoepoxides with dAdo. Characterization of adducts formed by isoprene monoepoxides with deoxynucleosides and subsequently with DNA represent the first step toward evaluating their potential for being converted into a mutation, or as biomarkers of isoprene metabolism and exposure.

INTRODUCTION

Isoprene, the 2-methyl analog of 1,3-butadiene, is an industrial chemical that has been classified as *possibly carcinogenic to humans (group 2B)* by IARC and as *reasonably anticipated to be a human carcinogen* by the National Toxicology Program. These conclusions are based on sufficient evidence from animal data (1–3), although to date, adequate epidemiological studies have not been available for categorization as a human carcinogen. Based on its abundance in cigarette smoke and its animal carcinogenicity, the World Health Organization has recently ranked isoprene third after 1,3-butadiene and acetaldehyde and similar to 4-(methylnitrosamino)- 1-(3-pyridyl)-1-butanone (NNK, one of the major tobacco-specific nitrosamines) with respect to cancer hazard stemming from smoking (4).

Like butadiene, isoprene is ubiquitous in the environment, with ambient air concentrations generally less than 10 ppb (0.030 mg/m^3) (3). The main sources of anthropogenic release of isoprene into the atmosphere are combustion processes (5–8).

In industry, isoprene is used as a monomer in the manufacture of synthetic rubber (*cis*-polyisoprene) and elastomers (copolymers with styrene or isobutene) (3). Occupational exposures to isoprene in the U.S. are usually less than 1 ppm (3 mg/m^3) as 8 h-time weighted average (9;10).

A significant contribution to total isoprene emissions stems from natural sources, since isoprene is a side product of several biological processes in plants, animals and bacteria (11;12). Human exposure to isoprene is largely due to its generation during endogenous processes, particularly isoprenoid biosynthesis, as it is the major hydrocarbon exhaled by humans (13). In summary, isoprene emissions from natural sources exceed those from industrial output by approximately 300-fold. Nevertheless, smoking increases isoprene exposure significantly and environmental tobacco smoke is the primary source of isoprene in indoor air (3;14).

Isoprene has been demonstrated to cause tumors in multiple organs in rodents, with mice being more sensitive than rats (15–18). Harderian gland and lung neoplasias developed in male mice after inhalation exposure to isoprene, and were linked to unique point mutations (A→T transversions) in the K-*ras* protooncogene at codon 61 (19;20).

Similar to its structural relative butadiene, isoprene is metabolized via oxidation by the cytochrome P450 enzymes, primarily CYP2E1, to the monoepoxides 2-ethenyl-2-methyloxirane (IP-1,2-O) and propen-2-yloxirane (IP-3,4-O). These can be further oxidized to the diepoxide (2-methylbioxirane) (21–23). The epoxides are hydrolyzed by epoxide hydrolase to the corresponding diol or epoxydiol isomers, or conjugated by glutathione-*S*-transferase (21–25).

Epoxides are reactive alkylating agents at nucleophilic sites of cellular macromolecules, including proteins and DNA. Formation of DNA adducts is believed to be the causal link between chemical exposures and mutagenesis and carcinogenesis (26;27). Chemical-specific DNA adducts are well established biomarkers for internal exposure and metabolism (28).

Unlike isoprene diepoxide, which was demonstrated to be mutagenic *in vitro* in *Salmonella typhimurium* strain TA100, neither the isoprene monoepoxides, nor the parent isoprene with or without metabolic activation were mutagenic in any *Salmonella* strains tested (15;29;30). However, with metabolic activation, IP-1,2-O and isoprene induced DNA strand breaks in human cells *in vitro* in the comet assay (31), thus demonstrating genotoxic potential.

To date, adduct formation of isoprene monoepoxides has been investigated in only a limited number of studies. This may be in part due to the negative outcome in the *in vitro* mutagenicity tests. Additionally, IP-1,2-O, thought to be the predominant metabolite based on i*n vitro* studies in rodent liver microsomes (23;32), is rapidly hydrolyzed in aqueous solution, thus probably preventing formation of adducts at biologically relevant levels. The half-lives of the monoepoxides in Tris-HCl buffer at physiological pH and temperature differ significantly: 1.25 hrs for IP-1,2-O compared to 73 hrs for IP-3,4-O (29). Bleasdale et al. (33) investigated the reactivity of IP-1,2-O with different nucleophiles *in vitro*. *In vivo*, adducts of both monoepoxides on the N-terminal valine of hemoglobin were detected in rats and mice following intraperitoneal administration of isoprene itself or a commercially available isoprene monoepoxide mixture, containing 95% IP-1,2-O and 5% IP-3,4-O (34). To date, the only studies investigating adducts of isoprene epoxides with DNA have been conducted by our group. In our previous *in vitro* study we demonstrated the formation of N7-guanine adducts after incubation of the 2′-deoxynucleotide or calf thymus DNA with isoprene monoepoxides (35).

In the present study, we investigated the generation of adducts from the reaction of the isoprene monoepoxides with 2′-deoxyadenosine (dAdo) (Scheme 1 and 2). Under physiological conditions, the major sites of adduct formation by alkyl epoxides on DNA bases are expected to be the endocyclic purine nitrogens, e.g. N3 and N1 of adenine, via an S_N2 mechanism. For epoxides with a vinyl or aryl substituent, such as styrene oxide and butadiene monoepoxide, direct adduct formation on exocyclic amino groups has also been reported (as reviewed in 36). In reactions of DNA with styrene and butadiene monoepoxides *in vitro*, N1-dAdo adducts have been identified, and evidence of their formation *in vivo* in humans was reported based on ^{32}P-postlabeling detection (37–39). N1-dAdo adducts tend to rearrange to N^6-dAdo adducts or to deaminate to the corresponding N1-deoxyinosine (dIno) adducts (38;40). We had a particular interest in the latter, because N1-dIno adducts of butadiene monoepoxide were demonstrated to be highly mutagenic in site-directed mutagenesis studies *in vitro* (41;42).

EXPERIMENTAL PROCEDURES

Caution

Epoxides are suspect carcinogens and should be handled with care

Chemicals

IP-1,2-O (2-ethenyl-2-methyloxirane, 2-methyl-2-vinyloxirane) was purchased from Aldrich Chemical Co. (Milwaukee, WI) as a 95:5 mixture with IP-3,4-O and will be referred to as $IPO_{commercial}$ (34). IP-1,2-O (> 99.8 %) was obtained through purification of $IPO_{commercial}$ by preparative GC on a Varian series 2700 gas chromatograph (Varian Instrument Division, Palo Alto, CA) equipped with a thermal conductivity detector. The column used was 2.5 m × 4 mm i.d., 10 % polyethylene glycol 20 M (Applied Science Laboratories Inc., State

College, PA); nitrogen was the carrier gas with a flow rate of 50 mL/min, the injection temperature was 20ºC, using a temperature gradient program starting at 20ºC, increasing 8°C/min to 150°C (t_R: 2.26 min) (Cottrell *et al.*, personal communication). IP-3,4-O (> 99 %) was synthesized and purified according to Harwood *et al.* (43).

The pure *S*-enantiomers of IP-1,2-O and IP-3,4-O were prepared as described (32). 2′-Deoxyadenosine (dAdo) and 2′-deoxyinosine (dIno) were purchased from Sigma Chemical Co. (St. Louis, MO). HPLC grade acetonitrile was purchased from Mallinckrodt Baker, Inc. (Paris, KY).

NMR Spectrometry

^{1}H NMR spectra were recorded at 500 MHz on a Varian INOVA 500 spectrometer (Palo Alto, CA) using 1–2 mg of the purified, lyophilized adducts dissolved in DMSO-d_6. Chemical shifts are reported in ppm relative to TMS. Heteronuclear Single Quantum Coherence (HSQC) and Heteronuclear Multiple Bond Correlation (HMBC) NMR experiments were performed on the Varian INOVA 500 spectrometer with ^{13}C signals acquired at 125 MHz. ^{1}H and ^{13}C signal assignments were made on the basis of Heteronuclear Single Quantum Coherence (HSQC) and Heteronuclear Multiple Bond Correlation (HMBC) NMR experiments.

HPLC analysis and purification

HPLC separations and purification were performed on reversed-phase (C18) Aquasil columns (Thermo Scientific, Raleigh, NC), using an Agilent Technologies (Palo Alto, CA) 1100 series quaternary pump, and a Hewlett Packard (Avondale, PA) 1040A diode-array detector (DAD) with HP Chem Station Software (Rev. A.05.04). Chromatograms were recorded with detector wavelengths set at 265 nm (between λ_{max} of the *N1*-dIno adducts (250 nm) and N^6-dAdo adducts (270 nm) and at 235 nm (to record the co-elution of byproducts). Additionally, UV spectra of HPLC peaks were recorded between 190 – 400 nm in 2 nm steps to confirm adduct identity. Mobile phases were: Mobile phase A, 17 mM ammonium acetate buffer (pH 5.5) containing 1.5% acetonitrile; mobile phase B, 17 mM ammonium acetate buffer (pH 5.5) containing 30% acetonitrile. Analytical separations were performed by injection of 80–100 μL of the reaction mixtures onto a 4.6 × 250 mm, 5 μm, 100 Å C18 Aquasil column with a flow of 1 mL/min. The linear gradient program was: 0–1 min 0% B, 1–60 min to 37% B, 60–80 min to 50% B (gradient program 1). Semipreparative separations were performed by injection of 0.5–1 mL amounts of the reaction mixtures onto a 10 × 250 mm, 5 μm, 100 Å C18 Aquasil column with a flow of 4 mL/min. The linear gradient program was: 0–1 min 0% B, 1–60 min to 37% B, 60–70 min to 45% B, 70–80 min 45% B (gradient program 2).

Liquid Chromatography-Electrospray Ionization-Mass Spectrometry (LC-ESI-MS)

LC-ESI-MS analyses were performed on an LCQ^{DECA} quadrupole ion trap mass spectrometer (Thermo Finnigan, San Jose, CA) equipped with an API2 electrospray ionization source operating in the positive ion mode. The heated transfer capillary temperature was kept at 350ºC. Nitrogen was used as both sheath and auxiliary gases and maintained at 80 and 20 arbitrary units, respectively. Spray voltage was 4.5 kV; collision energy was 20 eV. Reaction mixtures (10 μL) were analyzed by on-line LC-ESI-MS to acquire full scan ESI spectra. Online LC separations were carried out as described above for analytical HPLC conditions. A post-column split of the LC flow was accomplished using a T-connector to allow only about 1/3 (350 μL/min) of the LC effluent into the ESI source.

General Methods. 1. Reaction of dAdo or dIno with IP-1,2-O and IP-3,4-O

Solutions of dAdo or dIno were prepared by dissolving 20 μmol of the deoxynucleoside in 1 mL 50 mM phosphate buffer (pH 7.4). Aliquots of the solutions (200 μL) were transferred to glass vials with screw-top Teflon-coated caps and incubated with a 10-fold molar excess (4 μL) of either IP-1,2-O, *S*-IP-1,2-O, IP-3,4-O or *S*-IP-3,4-O in an Orbit environmental shaker (Lab-Line Instruments, Inc., Melrose Park, IL) at 37ºC for 24 h. The reaction mixtures were diluted 5-fold to 1 mL with doubly distilled water and extracted 3 times with equal volumes of diethyl ether to remove excess isoprene monoepoxide. Residual ether was evaporated from the reaction mixture under a stream of nitrogen at room temperature.

Under the analytical HPLC/LC conditions described above (4.6 × 250 mm C18 Aquasil column gradient program 1), reaction of dAdo with IP-1,2-O yielded several major products (Figure 1a), three of which were identified: **dAdo-1** (68.7 min, 2 partially resolved peaks), **dAdo-2** (73.4 min) and **dAdo-3** (74.5 min) (Table 1).

Under the same conditions, separation of the mixture from the reaction of dAdo with IP-3,4-O (Figure 2a) yielded the major products: **dAdo-6** (66.0 min), **dAdo-7** (69.2 min) and **dAdo-8** (71.6 min) along with five minor products: **Ade-1** (42.9 min), **dIno-2** (46.7 min), **dIno-3** (47.7 min), **dIno-4** (49.0 min), and **dIno-5** (50.7 min) (Table 1).

Mild acid hydrolysis—The deglycosylation of the dAdo and dIno adducts was performed at 80ºC for 1 h in 0.1 M HCl by adding an appropriate amount of 1 M HCl to the reaction mixture. The hydrolysates were neutralized with 2 M KOH.

Synthesis of dAdo and dIno Adducts of Isoprene Monoepoxides

dAdo was dissolved in 50 mM phosphate buffer (pH 7.4) (40 μmol/mL) by shaking at 37ºC for 1 h.

Either IP-1,2-O or IP-3,4-O in a 9-fold molar excess was added to the dAdo solution and the mixture was incubated in an Orbit environmental shaker at 37ºC for 3 days. The reaction mixture was either frozen or extracted immediately 3 times with 3 volumes of diethyl ether to remove excess isoprene monoepoxides and residual ether was evaporated from the reaction mixture under a nitrogen stream at room temperature. The reaction mixture was filtered through 0.2 μm Uniflo syringe filters (Schleicher & Schuell, Keene, NH) before separation by semi-preparative HPLC.

The fractions containing the major adducts were collected and dried in a Savant SVC100 Speed Vac (Thermo Savant, Milford, MA), and dissolved in a small amount of doubly distilled water. Fractions containing identical adducts were combined, lyophilized and characterized by NMR.

dAdo-1—^{1}H NMR (500 MHz, DMSO-d_6) 8.36, s, 1H, H8; 8.21, bs, 1H, H2; 7.16, bs, 1H, N^{6}*H*; partially resolved 6.35, dd, *J* = 7.7, 6.2 Hz, H1′ and 6.34, ψt. *J* = 7.0 Hz, H1′, total 1H; 5.93, dd, 1H, J=17.3, 10.7 Hz, H3^{IP}; 5.30, bd, 1H, J=3.1 Hz, 3′-O*H*; 5.24, dd, 1H, J=17.3, 1.9 Hz, C=C*H*$_2^{IP}$; 5.19, dd, 1H, J=11.5, 6.1 Hz, 5′-O*H*; 4.98, dd, 1H, J=10.7, 1.9 Hz, C=C*H*$_2^{IP}$; 4.41, m, 1H, H3′; 3.87, m, 1H, H4′; 3.62, dt, 1H, J=4.4, 11.4 Hz, H5′ or H5″; 3.57, bs, 1H, C*H*$_2^{IP}$; 3.55 – 3.49, m, 1H, H5″ or H5′; 2.73, m, 1H, H2″; 2.26, ddd, 1H, J=13.2, 7.0, 2.9 Hz, H2′; 1.18, s, 3H, C*H*$_3^{IP}$ ppm. ^{13}C NMR (125 MHz, DMSO-d^6) 152.3, C2; 148.2, C4; 144.0, C3^{IP}; 139.6, $^{1}J_{C\text{-}H}$=214.5 Hz, C8; 119.6, C5; 112.6, C=*C*H$_2^{IP}$; 88.0, C4′; 83.9, $^{1}J_{C\text{-}H}$=163.5 Hz, C1′; 72.4, C2^{IP}; 71.0, C3′; 62.1, C5′; 49.4, *C*H$_2^{IP}$; 39.6, C2′; 25.6, *C*H$_3^{IP}$ ppm.

dAdo-2—^{1}H NMR (500 MHz, DMSO-d_6) 8.36, s, 1H, H8; 8.19, s, 1H, H2; 6.78, s, 1H, N^{6}*H*; 6.34, dd, 1H, J= 7.6, 6.2 Hz, H1′; 6.10, dd, 1H, J= 17.6, 10.8 Hz, H3^{IP}; 5.38, bt, 1H, J=6.0 Hz, 1-O*H*^{IP}; 5.30, d, 1H, J=3.5 Hz, 3′-OH; 5.16, t, 1H, J=5.6 Hz, 5′-OH; 5.07, dd, J=17.6, 1.1 Hz, C=C*H*$_2^{IP}$; 5.05, dd, 1H, J=10.8, 1.1 Hz, C=C*H*$_2^{IP}$; 4.41, m, 1H, H3′; 3.88, m, 1H, H4′; 3.66 – 3.59, m, 2H, H5′ or H5″ and C*H*$_2^{IP}$; 3.54 – 3.48, m, 2H, H5″ or H5′ and C*H*$_2^{IP}$; 2.74, ddd, 1H, J=13.3, 7.6, 5.7 Hz, H2″; 2.26, ddd, 1H, 13.3, 6.2, 2.9 Hz, H2′; 1.55, s, 3H, C*H*$_3^{IP}$ ppm. ^{13}C NMR (125 MHz, DMSO-d_6) 154.2, C6; 151.7, $^{1}J_{C\text{-}H}$=200.5 Hz, C2; 148.0, C4; 141.8, $^{1}J_{C\text{-}H}$=156.0 Hz, C3^{IP}; 139.6, $^{1}J_{C\text{-}H}$=214.0 Hz, C8; 120.3, C5; 113.2, C=*C*H$_2^{IP}$; 87.9, C4′; 84.0, $^{1}J_{C\text{-}H}$=158.0 Hz, C1′; 71.0, C3′; 67.5, *C*H$_2^{IP}$; 61.9, C5′; 58.9, C2^{IP}; 39.5, C2′; 21.6, $^{1}J_{C\text{-}H}$=127.5 Hz, *C*H$_3^{IP}$ ppm.

dAdo-3—^{1}H NMR (500 MHz, DMSO-d_6) 8.36, s, 1H, H8; 8.19, s, 1H, H2; 6.78, s, 1H, N^{6}*H*; 6.34, dd, 1H, J= 7.6, 6.3 Hz, H1′; 6.10, dd, 1H, J= 17.6, 10.8 Hz, H3^{IP}; 5.39, bs, 1H 1-O*H*^{IP}; 5.32, bs, 1H, 3′-OH; 5.16, bt, 1H, J=~5 Hz, 5′-OH; 5.07, dd, J=17.6, 1.2 Hz, C=C*H*$_2^{IP}$; 5.05, dd, 1H, J=10.8, 1.2 Hz, C=C*H*$_2^{IP}$; 4.41, m, 1H, H3′; 3.88, m, 1H, H4′; 3.66 – 3.59, m, 2H, H5′ or H5″ and C*H*$_2^{IP}$; 3.54 – 3.48, m, 2H, H5″ or H5′ and C*H*$_2^{IP}$; 2.74, ddd, 1H, J=13.2, 7.6, 5.7 Hz, H2″; 2.26, ddd, 1H, 13.2, 6.3, 2.8 Hz, H2′; 1.54, s, 3H, C*H*$_3^{IP}$ ppm. ^{13}C NMR (125 MHz, DMSO-d_6) 154.2, C6; 151.7, $^{1}J_{C\text{-}H}$=200.5 Hz, C2; 148.0, C4; 141.8, $^{1}J_{C\text{-}H}$=156.0 Hz, C3^{IP}; 139.6, $^{1}J_{C\text{-}H}$=214.0 Hz, C8; 120.3, C5; 113.2, C=*C*H$_2^{IP}$; 87.9, C4′; 84.0, $^{1}J_{C\text{-}H}$=158.0 Hz, C1′; 71.0, C3′; 67.5, *C*H$_2^{IP}$; 61.9, C5′; 58.9, C2^{IP}; 39.5, C2′; 21.6, $^{1}J_{C\text{-}H}$=127.5 Hz, *C*H$_3^{IP}$ ppm.

dAdo-6—^{1}H NMR (500 MHz, DMSO-d_6) 8.35, s, 1H, H8; 8.18, s, 1H, H2; 7.54, d, 1H, *J* = 8.5 Hz, N^{6}*H*; 6.35, dd, 1H, *J* = 7.6, 6.2 Hz, H1′;5.31, d, *J* = 3.6 Hz, 1H 3′-OH; 5.21, t, 1H, *J* = 5.7 Hz, 5′-O*H*; 4.90, s, 1H, C=C*H*$_2^{IP}$; 4.80, m, 1H, H2^{IP}; 4.79, s, 1H, C=C*H*$_2^{IP}$; 4.74, bs, 1H, 1-O*H*^{IP}; 4.41, m, 1H, H3′; 3.88, m, 1H, H4′; 3.64, m, 2H, C*H*$_2^{IP}$; 3.62, m, 1H, H5′ or H5″; 3.51, m, 1H, H5″ or H5′; 2.73, ddd, 1H, *J* = 13.0, 7.6, 5.9 Hz, H2″; 2.26 (ddd, *J* = 13.06, 6.2, 2.8 Hz, 1H, H2′; 1.76, s, 3H, C*H*$_3^{IP}$ ppm. ^{13}C NMR (125 MHz, DMSO-d_6) 154.2, C6; 152.2, C2; 148.3, C4; 143.9, C3^{IP}; 139.3, $^{1}J_{C\text{-}H}$=212.0 Hz, C8; 119.7, C5; 111.2, C=*C*H$_2^{IP}$; 88.2, C4′; 83.8, C1′; 70.9, C3′; 57.0, C2^{IP}; 20.1, *C*H$_3^{IP}$ ppm

dAdo-7—^{1}H NMR (500 MHz, DMSO-d_6) 8.36, s,1H, H8; 8.18, s, 1H, H2; 7.54, d, 1H, $J_{NH\text{-}H3i}$ = 8.4 Hz, N^{6}*H*; 6.35, dd, 1H, *J*=7.4, 6.2 Hz, H1′; 5.30, d, 1H, *J*=4.0 Hz, 3′-O*H*; 5.20, dd, 1H, *J*=6.4, 5.1 Hz, 5′-O*H*; 4.89, s, 1H, C=C*H*$_2^{IP}$; 4.80, m, + 4.79, s, 2H, H2^{IP} + C=C*H*$_2^{IP}$, overlapping; 4.74, bs, 1H, 1-O*H*^{IP}; 4.41, m, 1H, H3′; 3.88, m, 1H, IP H4′; 3.64, m, 2H, C*H*$_2^{IP}$; 3.61, m, 1H, and 3.52, m, 1H, H5′, H5″; 2.72, ddd, 1H, J=13.2, 7.4, 6.0 Hz, H2″; 2.26, ddd, 13.2, 6.2, 2.8 Hz, 1H, H2′; 1.76, s, 3H, C*H*$_3^{IP}$ ppm. ^{13}C NMR (125 MHz, DMSO-d_6) 153.6, C6; 151.8, $^{1}J_{C\text{-}H}$=196.0 Hz, C2; 147.3, C4; 143.8, C3^{IP}; 139.1, $^{1}J_{C\text{-}H}$=212.0 Hz, C8; 118.9, C5; 111.1, C=C*H*$_2^{IP}$; 87.8, C4′; 84.1, C1′; 70.8, C3′; 61.5, C*H*$_2^{IP}$; 61.4, C5′; 56.6, C2^{IP}; 19.8, $^{1}J_{C\text{-}H}$=125.5 Hz, *C*H$_3^{IP}$ ppm.

dAdo-8—^{1}H NMR (500 MHz, DMSO-d_6) 8.34, s, 1H, H8; 8.21, s, 1H, H2; 7.44, bs, 1H, N^{6}*H*; 6.34, dd, 1H, *J* = 7.6, 6.3 Hz, H1′; 5.32, bs, 1H, 3′-O*H*; 5.21, bs, 1H, 5′-O*H*; 4.90, bs, 1H, C=C*H*$_2^{IP}$; 4.77, bs, 1H, C=C*H*$_2^{IP}$; 4.41, td, 1H *J* = 5.4, 2.8, 2.6 Hz, H3′; 4.20 bt, 1H, *J* = 5.4, Hz, H2^{IP}; 3.88 m, 1H, H4′; 3.62, dd, 1H, *J* = 11.8, 4.2 Hz, and 3.52, dd, 1H, *J* = 11.8, 4.2 Hz, H5′, H5″; 3.65, bs, 1H, C*H*$_2^{IP}$; 3.46, bs, 1H, C*H*$_2^{IP}$; 3.33, bs, 1H, 2-O*H*^{IP}; 2.72, ddd, 1H, *J* = 13.2, 7.6, 6.0 Hz, H2″; 2.26, ddd, 1H, *J* = 13.2, 6.3, 2.9 Hz, H2′; 1.72, s, 3H, C*H*$_3^{IP}$ ppm. ^{13}C (125 MHz, DMSO-d_6) 153.9, C6; 152.0, $^{1}J_{C\text{-}H}$=199.5 Hz, C2; 148.0, C4; 146.3, C3^{IP}; 139.3, $^{1}J_{C\text{-}H}$=219.0 Hz, C8; 119.5, C5; 111.0, C=*C*H$_2^{IP}$; 87.6, C4′; 83.5, C1′; 72.6, C2^{IP}; 70.6, C3′; 61.5, C5′; 44.3, *C*H$_2^{IP}$; 39.6, C2′; 17.7, *C*H$_3^{IP}$ ppm.

dIno-2—^{1}H (500 MHz, DMSO-d_6) 8.31, s 1H, H8; 8.25, s, 1H, H2; 6.30, dd, 1H, J = 7.2, 6.5 Hz, H1′; 5.33, dd, 1H, J = 7.5, 4.5 Hz, 3′-O*H*; 4.99, t, 1H, J = 5.4 Hz, 5′-O*H*; 4.91, s, 1H, C=CH_2^{IP}; 4.84, s, 1H, C=CH_2^{IP}; 4.39, m, 1H, H3′; 4.24 dd, 1H, J = 13.1, 3.9 Hz, CH_2^{IP}; 4.17, m, 1H, H2^{IP}; 3.86, dt, 1H, J = 4.6, 3.1 Hz, H4′; 3.76, dd, 1H, J = 13.1, 8.4 Hz, CH_2^{IP}; 3.59, td, 1H, J = 11.35, 4.6 Hz, H5′ or H5″; 3.54–3.49, m, 1H, H5″ or H5′; 2.62, ddd, 1H, J = 13.3, 7.2, 6.11 Hz, H2″; 2.30, ddd, 1H, J = 13.3, 6.5, 3.3 Hz, H2′; 1.78, s, 3H, CH_3^{IP} ppm. ^{13}C (125 MHz, DMSO-d_6) 156.0, C6; 149.2, $^{1}J_{C\text{-}H}$=208.0 Hz, C2; 147.1, C4; 145.4, C3^{IP}; 138.9, $^{1}J_{C\text{-}H}$=215.0 Hz, C8; 123.7, C5; 111.5, C=CH_2^{IP}; 88.0, C4′; 83.5, C1′; 71.3, C2^{IP}; 70.6, C3′; 61.7, C5′; 49.9, CH_2^{IP}; 39.7, C2′; 18.2, CH_3^{IP} ppm

dIno-5—^{1}H (500 MHz, DMSO-d_6) 8.33, s, 1H, H8; 8.23, s, 1H, H2; 6.31, 1H, t, J = 6.8, Hz, H1′; 5.36, m, 1H, H2^{IP}; 5.11, bs, 1H, 3′-O*H*; 5.07, m, 1H, C=CH_2^{IP}; 4.98, m 1H, 5′-O*H*; 4.92. m, 1H, C=CH_2^{IP}; 4.39, m, 1H, H3′; 3.99, CH_2^{IP}; 3.90 – 3.84, m, 2H, CH_2^{IP} + H4′; 3.62 – 3.56, 1H, H5′ or H5″; 3.54 – 3.48, m, 1H, H5″ or H5′; 2.65, ddd, 1H, J = 13.3, 6.8, 5.9 Hz, H2″; 2.31, ddd, J = 13.3, 6.8, 3.3 Hz, 1H, H2′; 1.67, CH_3^{IP} ppm. ^{13}C (125 MHz, DMSO-d_6) 156.3, C6; 146.7, C4; 146.6, $^{1}J_{C\text{-}H}$=207.0 Hz, C2; 141.2, C3^{IP} 139.1, $^{1}J_{C\text{-}H}$=214.5 Hz, C8; 123.5, C5; 114.1, $^{1}J_{C\text{-}H}$=156.0 Hz, C=CH_2^{IP}; 88.1, C4′; 83.5, $^{1}J_{C\text{-}H}$=164.5 Hz, C1′; 70.8, C3′; 61.8, C5′; 60.4, CH_2^{IP}; 58.4, C2^{IP}; 39.9, C2′; 20.7, $^{1}J_{C\text{-}H}$=127.0 Hz, CH_3^{IP} ppm.

Ade-1—^{1}H (500 MHz, DMSO-d_6) 8.32, s, 1H, H8; 8.18, s, 1H, H2; 6.74, s, 2H, N^6*H*; 5.33, bs, 1H, 1-OH^{IP}; 5.28, dd, 1H, J = 7.5, 3.5 Hz, H2^{IP}; 5.02, m, 1H, C=CH_2^{IP}; 4.75, m, 1H, C=CH_2^{IP}; 4.08, ddd, 1H, J = 10.9, 7.5, 2.9 Hz, CH_2^{IP}; 3.97, m, 1H, CH_2^{IP}; 1.65, CH_3^{IP} ppm. ^{13}C (125 MHz, DMSO-d_6) 159.6, C4; 152.0, $^{1}J_{C\text{-}H}$=198.0 Hz, C2; 151.7, C6; 144.5, $^{1}J_{C\text{-}H}$=210.5 Hz, C8; 142.1, C3^{IP}; 113.9, C=CH_2^{IP}; 111.6, C5; 63.0, C2^{IP}; 19.9, $^{1}J_{C\text{-}H}$=127.0 Hz, CH_3^{IP} ppm.

RESULTS

Identification and Characterization of Adducts Resulting from the Reaction of Racemic Isoprene Monoepoxides with dAdo

General considerations in structural assignments—In addition to regioisomers resulting from addition of dAdo at the internal and terminal oxirane carbons of the IP oxides, diastereomers of the N9-deoxyribosyl adducts and racemic mixtures of deglycosylated bases are possible as a result of the asymmetry at the internal sp^3 carbon of the side-chain derived from ring-opening of an isoprene epoxide.

As described below, the availability of the pure *S*-enantiomers of IP-1,2-O and IP-3,4-O allowed a number of adducts to be characterized to the level of absolute configuration, under the assumption that opening of the oxirane occurs predominantly via an S_N2-mechanism with inversion of configuration at the chiral center. Products were tentatively identified as dAdo or N1-dIno adducts by comparison of UV spectra acquired by diode array scans with spectra of structurally similar adducts (37;44–46). The UV spectra of the N1-dIno adducts of isoprene monoepoxides have a maximum at 250 nm with a characteristic shoulder at ~273 nm (Figure 3a), while a shoulder is absent from the spectra of the N1-and N^6-dAdo adducts (Figure 3b, spectra not shown for *N1*-dAdo adducts), which are characterized by symmetrical maxima at 260 and 265–270 nm, respectively. Confirmation of assignments based on UV-vis spectra was derived from comparison of chromatograms of dAdo-isoprene monoepoxide reaction mixtures with those of dIno-isoprene monoepoxide reaction mixtures (Figures 2 & S1).

Support for the assignments of adducts as dAdo or dIno adducts was also provided by LC-ESI-MS/MS analysis of the reaction mixtures in full scan mode with simultaneous DAD

detection using chromatographic conditions identical to those of the analytical HPLC-DAD analysis. Isoprene-derived dAdo and dIno adducts fragment similarly to other DNA adducts and nucleosides (47): the full scan mass spectra of dAdo adducts were characterized by a series of ions at *m/z* 336 (MH^+), 220 ($[MH - dR]^+$), 136 ($[MH - dR - C_5H_9O]^+$), and the dIno adduct mass spectra by ions at *m/z* 337 (MH^+), 221 ($[MH - dR]^+$), 137 ($[MH - dR - C_5H_9O]^+$) (Table 1). Furthermore, it was shown that adducts derived by attack either on the external or internal oxirane carbon of isoprene monoepoxides have distinctly different fragmentation patterns in the MS/MS of the ion corresponding to $[MH - dR]^+$ (Table 1, Figures 4 and S2 & S3, Schemes S1 & S2).

Both ^1H NMR and 2D homo- and heteronuclear shift correlation spectra completed the structural assignments. A number of features of the NMR spectra were generally applicable in interpreting NMR data. Although diastereomers are, in principle, different compounds - and several of the diastereomeric adducts were completely resolved by HPLC - the proton and carbon shifts of the diastereomers were virtually identical and differences in ^1H and ^{13}C chemical shifts could be resolved for only a few signals. Shift assignments of carbon and proton signals of the deoxyribose (dR) moiety could be readily made on the basis of comparison with published coupling patterns and hyperfine shifts in the ^1H NMR spectra (48) and C,H coupling in the single- and multiple-bond shift correlation spectra (HSQC and HMBC, respectively). The proton and carbon signals of the base moieties of adducts were similarly assigned (complete 2D spectra are provided in Figures S4 – S21). In all HMBC spectra, unsuppressed one-bond couplings $^1J_{C,H}$ were observed at C8 and the isoprenyl side-chain methyl group (the term 'isoprenyl' refers to the C5 unit derived from ring-opening of an isoprene epoxide). Unsuppressed one-bond couplings at purine C2 and deoxyribose C1′ were also observed for most adducts. The magnitudes of the one-bond couplings were uniformly in accord with expectation (49), and useful in supporting signal assignments. Two- and three-bond couplings were observed between the isoprenyl methyl protons and the methyl-substituted and adjacent isoprenyl backbone carbons, providing unequivocal assignment of three of the four isoprenyl side-chain carbons. With the exception of product **Ade-1**, the deglycosylated N7 adduct, straightforward assignment of the remaining isoprenyl carbon signal was made from HSQC and HMBC data.

As indicated in the structural diagrams, the numbering convention applied to the isoprenyl side-chain of adducts is assignment of position 1 to the carbon closest to the point of attachment to the base. As a result, the isoprenyl backbone carbons are renumbered in the adducts of IP-3,4-O. Assignment of the proton and carbon signals of the isoprenyl side-chains allowed determination of the points of attachment on both the isoprenyl side-chain and base. In the case of products **dIno-2**, **dIno-5**, **dAdo-7**, **dAdo-2**, and **dAdo-3**, the regiochemistry of addition could be determined unambiguously through connectivity observed between the side-chain and the base in the heteronuclear shift correlation spectra. For the remaining adducts, substituent effects on ^{13}C chemical shifts of the IP side-chain carbons were important in rigorous structural assignments. Nucleophilic attack at the terminal oxirane carbon of IP-3,4-O will result in an aminohydrin adduct in which the internal carbon ($C2^{IP}$) bears both hydroxyl and vinyl substituents, resulting in a strong downfield carbon shift for this carbon atom (50). For adducts at the terminal carbon, $C2^{IP}$ is therefore expected to show a substantial downfield shift relative to $C1^{IP}$. By contrast, the aminohydrin from attack at the internal oxirane carbon bears the hydroxyl substituent on $C1^{IP}$ and the shifts of $C1^{IP}$ and $C2^{IP}$ are nearly identical. This behavior has been reported for the isoprene adducts of Gua (35), in which addition at the terminal oxirane carbon results in a shift of $C2^{IP}$ >10 ppm downfield relative to $C1^{IP}$, while the separation of signals is < 3 ppm for adducts at the internal carbon. The shifts of the terminal ($C4^{IP}$) and internal ($C3^{IP}$) vinylic carbons also behave in accord with expectation, with the internal vinyl carbon signals appearing >20 ppm downfield of the terminal vinyl carbon signals. The HMBC and

HSQC spectra recorded for the dIno-5 adduct in Figure 5 illustrate the NMR features that were helpful in making structural assignments.

Adducts of IP-1,2-O: The major adducts of *racemic*-IP-1,2-O (*rac*-IP-1,2-O) were two sets of diastereomers formed by addition of the exocyclic amino group of dAdo at the terminal (C1) and internal (C2) oxirane carbons (the numbering of the isoprene side-chain does not change for IP-1,2-O adducts). Adducts were collected by semipreparative HPLC in three major peaks (**dAdo-1, dAdo-2, dAdo-3**), having UV-vis spectra characteristic of N^6-dAdo adducts (Figure 3b). On an analytical HPLC column, **dAdo-1** appeared to contain unresolved components (Figure 1a).

Analysis of the reaction mixture by LC-MS yielded mass spectra consistent with dAdo adducts (Figure 4) for all three peaks. MS/MS of the ion at *m/z* 220, present in all three mass spectra, showed loss of H2O in the case of the **dAdo-1** mixture and loss of the isoprenyl moiety for **dAdo-2** and **dAdo-3** based on the resulting fragment ions *m/z* 202 and *m/z* 136, respectively (Figure 4). The fragmentation patterns are in accord with diastereomeric pairs from two regioisomers. The transition state stabilization by allylic resonance should favor loss of H2O from the secondary alcohols arising via addition at the terminal oxirane carbon, while loss of the isoprenyl moiety by breaking of the bond to the purine would be favored from adducts derived by attack at the internal oxirane carbon (Scheme S1). Thus, **dAdo-1** is comprised of partially resolved terminal oxirane adducts and **dAdo-2** and **-3** represent adducts at internal oxirane carbons.

Mild acid hydrolysis of the dAdo-*rac*-IP-1,2-O reaction mixture gave two major product peaks that corresponded in their fragmentation patterns of the MS/MS of the ion at *m/z* 220 to those of the regioisomeric pairs of N^6-dAdo adducts, which must therefore be racemic mixtures of the deglycosylated adducts at terminal and internal oxirane carbons, respectively (Figure 1b). Also consistent with the assignment of the dominant products as two sets of diastereomers, are the observations that the major dAdo-*S*-IP-1,2-O adducts (Figure S22) co-chromatograph with **dAdo-1**, and **dAdo-2** and have identical ESI-MS/MS fragmentation patterns. On this basis, **dAdo-2** and **dAdo-3** can be assigned to the diastereomeric adducts at the internal oxirane carbon of the *R*-, and *S*-IP-1,2-O enantiomers, respectively, and **dAdo-1** to an unresolved mixture of diastereomeric adducts at the terminal carbon.

The ^{1}H NMR spectra establish that **dAdo-1**, **dAdo-2** and **dAdo-3** are adducts at the exocyclic amino group of dAdo on the basis of one-proton singlets at hyperfine shifts expected for $N^6\underline{H}$, 7.16 ppm for **dAdo-1** (Figures S4, S5) and 6.79 ppm for **dAdo-2** and **dAdo-3** and confirmed as amino protons by the absence of C,H correlations for these signals in the HSQC spectra (Figures S6, S7). (^{1}H and ^{13}C chemical shifts of **dAdo-2** and **dAdo-3** were identical and the fractions were combined and analyzed as a mixture for 2D NMR to improve the quality of the spectra.) The suggestion that **dAdo-1** is probably a mixture of diastereomers, is supported by partial resolution of two H1′ signals in the ^{1}H NMR spectrum (Figures S4, S5). Resolution of two sets of diastereotopic methylene signals at C1^{IP}, adjacent to the stereogenic center, which are also expected to be highly sensitive to structural differences induced by differing configurations at C1′ and C2^{IP}, was precluded by overlap with H5′,H5″ signals. The ^{13}C and the remaining ^{1}H shifts of the diastereomers were identical. Although no C,H correlations could be detected between the isoprenyl side-chain and the purine base in the HMBC spectrum, the assignment of the **dAdo-1** mixture as regioisomers from addition at the terminal oxirane carbon of IP-1,2-O is established by the large chemical shift difference between C1^{IP} and C2^{IP}. The signal corresponding to C1^{IP} at 49.4 ppm is established by a cross peak with the isoprenyl methyl protons at 1.18 ppm in the HMBC spectrum. The signal for C2^{IP} is identified at 72.4 ppm by cross peaks with H3^{IP} at 5.93 ppm and the terminal methylene protons at 4.98 and 5.24 ppm. The C1^{IP} – C2^{IP} shift

difference of 23.0 ppm for **dAdo-1** compared to 9.0 ppm for **dAdo-2** and **dAdo-3** (vide infra) is consistent with the assignment of **dAdo-1** as the adduct at the terminal oxirane carbon. **dAdo-2/dAdo-3** are unequivocally assigned as adducts at the internal oxirane carbon by the HMBC spectrum: there are cross peaks between $N^6\underline{H}$ and both the isoprenyl methyl carbon at 21.6 ppm and a carbon at 58.9 ppm, assigned to methyl-substituted $C2^{IP}$ based on 2-bond coupling with the isoprenyl methyl protons and no attached proton, indicated by the absence of a C,H correlation in the HSQC spectrum. In the HSQC spectrum, $C1^{IP}$ appears at 67.9 ppm, and as discussed above, the $C1^{IP} – C2^{IP}$ shift difference of 9 ppm relative to 23.0 ppm for **dAdo-1** is in accord with this assignment. Thus, **dAdo-2** can be characterized as the N^6-2-*R*- and **dAdo-3** as the N^6-2-*S*-isopropenyl adducts of dAdo. See Table 1 for complete structural assignments.

Adducts of IP-3,4-O: HPLC separation of the dAdo-*rac*-IP-3,4-O reaction mixture yielded a total of nine products in sufficient quantity to characterize by UV-vis and full scan mass spectra (Figure 2a). In this manner, three major products could be identified as dAdo adducts **dAdo-6**, **dAdo-7, dAdo-8** and four minor products as dIno adducts **dIno-2**, **dIno-3**, **dIno-4**, **dIno-5**. The identity of the dIno adducts was confirmed by co-chromatography with reaction products of dIno with IP-3,4-O (Figure S1a). The retention times of two additional products were shorter than the dAdo and dIno adducts and did not change following mild acid hydrolysis of the reaction mixture, implying that they are deglycosylated adducts (Figure 2b). This conclusion was supported by full scan mass spectra which contained no ions corresponding to adducted nucleosides and by UV-vis spectra, which were similar to those reported for N3- and N7 adducts of Ade with butadiene monoepoxide (37).

dAdo adducts—In the MS/MS of the ion at *m/z* 220, **dAdo-8** readily loses water and 2-methylpropenol based on the major product ions *m/z* 202 and *m/z* 148, respectively (Figure S2A). In the MS/MS of *m/z* 220 from **dAdo-6** and **dAdo-7** loss of the isoprenyl side-chain along with loss of H_2O accounted for the product ions *m/z* 136 and *m/z* 136 (Figure S2B). Loss of 2-methylpropenol unit could only occur from the adduct at the terminal position of IP-3,4-O, while formaldehyde might be expected from the adduct at the internal carbon. The mass spectra therefore support **dAdo-8** as a mixture of diastereomers at the terminal carbon and **dAdo-6** and **dAdo-7** as adducts at the internal carbon of IP-3,4-O.

As expected for pairs of diastereomers, mild acid hydrolysis of the reaction mixture from dAdo and *rac*-IP-3,4-O yielded two major deglycosylation products (Figure 2b), which corresponded in their fragmentation patterns of the MS/MS of the ion at *m/z* 220 to those of the regioisomeric pair of N^6-dAdo adducts. Major products of the reaction of dAdo with *S*-IP-3,4-O co-chromatographed with **dAdo-7** and **dAdo-8**. Under the assumption of an S_N2 reaction, the adducts at the internal oxirane carbon, **dAdo-7** and **dAdo-6** can be assigned *R* and *S* configurations, respectively, at $C2^{IP}$. The contribution to the **dAdo-8** mixture from addition to the terminal oxirane carbon of *S*-IP-3,4-O has *S* configuration at $C2^{IP}$ (Figure S21).

In ^{1}H NMR spectra of the three fractions, one-proton signals corresponding to $N^6\underline{H}$ indicate attachment of the isoprenyl chain to dAdo at the exocyclic amino group. The identity of $N^6\underline{H}$ was confirmed by absence of a cross peak with carbon in the HSQC spectra. The ^{1}H shifts of **dAdo-6** and **dAdo-7** are virtually identical (Figures S8 – S12). The quantity of **Ado-6** collected was significantly smaller than **dAdo-7**, precluding the establishment of connectivity between the C4 chain and the base in the C,H shift correlation experiments. The observable carbon shifts of **dAdo-6** were identical to the corresponding signals of **dAdo-7.** Based on the similarity of the ^{1}H and ^{13}C shifts, **dAdo-6** and **dAdo-7** are diastereomers, and assignment of the regiochemistry of addition described below for **dAdo-7** applies to both products.

The shifts of deoxyribose C5′ and the terminal sp^3 methylene ($C1^{IP}$) of the isoprenyl side-chain (61.5 ppm) are identical, but are assigned by resolution of the proton signals in the HSQC spectrum (Figure S11). The internal isoprenyl sp^3 carbon $C2^{IP}$signal can be assigned at 56.6 ppm by virtue of cross peaks with the isoprenyl methyl protons at 1.76 ppm and vinyl methylene C4H2IP at 4.79 ppm. The shift difference of 4.9 ppm between $C1^{IP}$ and $C2^{IP}$ suggests addition at the internal oxirane carbon, which is consistent with the appearance of $N^6\underline{H}$ as a doublet, coupling with $H2^{IP}$. The absence of a cross peak for expected 2-bond connectivity between $C2^{IP}$ and N^6H can probably be ascribed to broadening of this signal. However, a cross peak between $H2^{IP}$ and N^6H in the DFQC spectrum (Figure S12) confirms the $N^6\underline{H}$-$C2^{IP}$ coupling and the structural assignment of addition at the internal oxirane carbon. In the HPLC trace of the products from reaction of 3*S*-IP-3,4-O with dAdo one of the major products co-elutes with **dAdo-7**. Taking into account that **dAdo-7** and **dAdo-6** are diastereomers and assuming that oxirane ring opening occurs with inversion of configuration at $C2^{IP}$, **dAdo-7** is assigned as the 2*R* diastereomer and **dAdo-6** as the 2*S* diastereomer from adduct formation at the internal oxirane carbon, consistent with the conclusion above based on comparison of the HPLC traces obtained from the reaction of dAdo with *S*-IP-3,4-O and with *rac*–IP-3,4-O.

In the HMBC spectrum of **dAdo-8** (Figure S13) from the reaction of *rac*-IP-3,4-O, connectivity was not observed between the isoprenyl side-chain and the base. This may be a consequence of broadening of H2, $N^6\underline{H}$, $H2^{IP}$ and the diastereotopic $C1^{IP}$ methylene signals as a result of imino-amino tautomerism of the purine or rotational isomerization about the N^6-isoprenyl bond on a time scale approaching the NMR time frame. Additionally, while **dAdo-8** from *rac*-IP-3,4-O is expected to be a mixture of diastereomers, neither the proton nor carbon signals at the 1′ and 2^{IP}positions were resolved into multiple signals, although these should be most sensitive to the differences in configuration at the stereogenic centers. In the HSQC spectrum (Figure S14), $C1^{IP}$ and $C2^{IP}$ appear at 44.5 and 72.6 ppm, respectively. The separation of 28.1 ppm between $C1^{IP}$ and $C2^{IP}$ is consistent with attachment at the terminal oxirane carbon, and is also in accord with the loss of water and 2-methylpropenol in the MS^2 of the deglycosylated product ion. An adduct of *S*-IP-3,4-O and dAdo co-chromatographs with **dAdo-8**, indicating that the 3*S* diastereomer contributes to **dAdo-8**. Based on the observation that the NMR data do not appear to distinguish between diastereomers of dAdo adducts in a definitive manner (vide infra), **dAdo-8** is assigned as a mixture of the diastereomeric adducts at the terminal oxirane carbon. See Table 1 for complete structural assignments.

dIno adducts—dIno-2, dIno-3, dIno-4, and dIno-5, were identified as dIno adducts by exact mass measurements of the protonated molecules, full scan ESI-MS and UV-vis. Definitive assignment as dIno adducts was further confirmed by co-chromatography with the reaction products of dIno with *rac*-IP-3,4-O (Figures 2a, S1a). Comparison of HPLC traces of the reaction mixtures from dAdo and dIno with *rac*- and *S*-IP-3,4-O indicated that **dIno-2** and **dIno-4** were adducts of *S*-IP-3,4-O (Figures S23, S24). The pairs **dIno-2**/**dIno-3 and dIno-4**/**dIno-5** displayed distinct differences in abundance of ESI-MS/MS fragments of *m/z* 221 and could therefore be assigned as diastereomeric pairs of regioisomeric adducts. The major product ion of **dIno-2**/**dIno-3** (*m/z* 203) resulted from loss of H2O, while **dIno-4** and **dIno-5** fragmented predominantly to *m/z* 137 through loss of the isoprenyl side-chain. In addition to the N^6-Ade adducts described above, mild acid hydrolysis of the reaction mixture of dAdo and *rac*-IP-3,4-O yielded a pair of hypoxanthine adducts (deglycosylated dIno adducts) with retention times similar to those observed after mild acid hydrolysis with *rac*-IP-3,4-O adducts of dIno (Figure 2b, Figure S1b). Furthermore, the two hypoxanthine adducts corresponded in their MS/MS fragmentation patterns of the ion at *m/z* 221 to those of the regioisomeric pairs of the dIno adducts. Although only **dIno-2** and **dIno-5** were collected in sufficient quantity for characterization by NMR (Figures S15 – S18), the

relation of **dIno-2** and **dIno-3** as 2^{IP}-*S*- and 2^{IP}-*R* diastereomers from addition at the terminal oxirane carbon and **dIno-4** and **dIno-5** as the 2^{IP}-*R*- and 2^{IP}-*S*- diastereomers from addition at the internal oxirane carbon allowed complete structural assignment of all four dIno adducts. It is worthy of comment that reaction of *S*-IP-3,4-O with dAdo yielded a the single predominant diastereomer, dIno-4, identified (vide infra) as the adduct at the internal oxirane carbon. Similarly, the reaction of *S*-IP-3,4-O yielded dIno-2 and dIno-4 as the predominant diastereomers. The absence of dIno-3 and dIno-5 as significant products indicates little or no racemization during substitution at either oxirane carbon, implying that an S_N2 reaction mechanism predominates. If reaction at the internal oxirane carbon had proceeded by an S_N1 mechanism (36) via an intermediate allylic cation, this should have resulted in racemization at $C2^{IP}$ to yield ~ equal proportions of adducts at the internal oxirane carbon, dIno-4 and dIno-5.

The absence of imino N*H* signals in the ^{1}H NMR spectrum supported substitution at N1. **dIno-2** was assigned as the N1 adduct at the terminal oxirane carbon based on the following evidence. The two sp^3 carbon signals of the isoprenyl side-chain appear at 49.9 and 71.3 ppm. The ~21 ppm separation is consistent with attachment at the terminal oxirane carbon, which is confirmed by a cross peak in the HMBC spectrum between the carbon signal at 49.9 ppm and H2 of dIno, strong 3-bond coupling between the diastereotopic methylene proton signal at 3.76 ppm and C2 and C6 of dIno and weak 4-bond coupling between $H2^{IP}$ and dIno C2 and C6. Consistent with assignment of **dIno-5** as the product of addition to the internal oxirane carbon, the two sp^3 carbon signals of the isoprene side-chain appear at 58.4 and 60.4 ppm, separated by only 2 ppm. Cross peaks in the HMBC spectrum between $H2^{IP}$ at 5.37 ppm and C2 and C6 of dIno at 146.6 and 156.3 ppm, respectively, confirm $C2^{IP}$ as the point of attachment, with additional support from observation of the corresponding cross peak between H2 of dIno at 8.23 ppm and $C2^{IP}$ at 58.4 ppm (Figure S17). See Table 1 for complete structural assignments.

N7-Ade adduct—Of the two product peaks tentatively identified as N3- or N7-Ade adducts based on UV-vis and mass spectra, only **Ade-1** (see Figure 3c for UV spectra,) was collected in sufficient quantity for NMR characterization (Figures S19 – S21), although the set of heteronuclear shift correlations observed was incomplete. The absence of C,H correlations of the diastereotopic methylene protons allowed identification of only three isoprenyl backbone carbon signals. In the ^{1}H NMR spectrum, a two-proton singlet at 6.74 ppm with no C,H correlation in the HSQC spectrum and a cross peak with C5 in the HMBC spectrum can be assigned to the exocyclic amino protons, ruling out attachment at N^6. A carbon at 63.0 ppm having cross peaks with the terminal vinyl methylene protons at 4.08 and 3.97 ppm and the isoprenyl methyl protons at 1.65 ppm can be assigned to $C2^{IP}$. The shift suggests that $C2^{IP}$ is the point of attachment of the base to the isoprenyl side-chain, since a shift of ~ 70 ppm would be predicted for $C2^{IP}$ if the point of attachment were at $C1^{IP}$. The attachment of the isoprenyl side-chain at $C2^{IP}$ is confirmed by the HMBC spectrum in which $H2^{IP}$ has a cross peak with C8 of Ade. The NOESY spectrum (Figure S21) demonstrates N7 rather than N3 as the site of attachment to the base. NOESY cross peaks are observed between H8 and the isoprenyl methyl, one of the diastereotopic methylene protons, one of the terminal vinyl methylene protons and $H2^{IP}$, which would not be possible for an N3 adduct. Based on the NMR analysis, **Ade-1** is assigned as the racemic N7-Ade adduct from attack at the internal oxirane carbon of IP-3,4-O. See Table 1 for complete structural assignment.

DISCUSSION

Isoprene is carcinogenic in mice and rats. Its mode of action is thought to be via metabolic activation and formation of pro-mutagenic DNA adducts that subsequently result in

mutagenesis and tumorigenesis. We have previously reported formation of guanine adducts by isoprene monoepoxides (35). However, isoprene-induced tumors in mice show unique point mutations (A→T transversions) in the K-*ras* protooncogene (19;20). Consequently we extended our investigation to the reaction of the two monoepoxides of isoprene with 2′-deoxyadenosine. We present here for the first time the characterization of adducts formed by isoprene monoepoxides with dAdo under physiological conditions. Major stable adducts of each monoepoxide were identified by HPLC, UV-Spectrometry and LC-MS and characterized by ^{1}H and $^{1}H,^{13}C$ HSQC and HMBC NMR experiments.

We demonstrated formation of regioisomeric N^6-dAdo adducts with both monoepoxides and formation of *N1*-dIno adducts with IP-3,4-O. In addition the reaction with IP-3,4-O also formed significant amounts of an N7-Ade adduct, stemming from deglycosylation of the unstable N7-dAdo adduct (51). Difficulties in characterizing the minor products of IP-1,2-O were due to its tendency for rapid hydrolysis in aqueous solution (29;52). This instability of IP-1,2-O lies in the direct attachment of the methyl group to the oxirane ring enhancing S_N1 attack at the internal oxirane carbon by a nucleophile such as water (52). Therefore, reactions with IP-1,2-O yielded smaller amounts of adducts compared to IP-3,4-O.

Besides N^6-dAdo and N1-dIno adducts, N1-dAdo were expected to form under the study conditions. It should be noted however, that we did not attempt to identify N1-dAdo adducts, because they readily rearrange or deaminate to the corresponding stable N^6-dAo and N1-dIno adducts, respectively (38;40). In biomarker studies, stable adducts are essential to increase reproducibility and N1-Ade adducts have been converted to N^6-adducts for analysis (39).

Adducts that we could tentatively identify as N1-dAdo adducts based on retention times that were similar to dAdo, and their UV spectra (λ_{max} = 260) (44–46), were not detectable when the incubation time was extended from 1 day to 3 days. Therefore, to increase yields of the stable adducts, dAdo was incubated for 3 days with each monoepoxide. Structural assignments made by UV and MS were confirmed by NMR. Diastereomeric assignments were made based on the fact that adduct formation by a S_N2 mechanism on the internal (stereogenic) oxirane carbon leads to a inversion of configuration, whereas adduct formation by S_N2 mechanism on the terminal oxirane carbon does not affect configuration on the stereogenic (internal) oxirane carbon. Steric effects favor S_N2 reaction at the terminal carbon, whereas substituents on the internal carbon that can stabilize positive charge favor reaction at the internal carbon by either S_N1 or S_N2 mechanisms (36). The assignment of a S_N2 mechanism to adducts at the internal oxirane carbons of the isoprene oxides is based on the observation that pure *S*-IP-1,2-O and *S*-IP-3,4-O yielded predominantly single diastereomers (**dAdo-2** and **dAdo-7**, **dIno-2** and **dIno-4,** respectively) rather than diastereomeric mixtures expected to result from S_N1 reaction. The requirement for a stereoselective process thus suggests adduct formation predominantly through a S_N2 rather than a S_N1 pathway, although adduct formation at the internal oxirane carbon of the IP-1,2-O is sterically hindered and has been proposed to occur through a S_N1 (or S_N1-like) mechanism, as also suggested for N7-guanine adducts of isoprene monoepoxides (35). Whereas simple mono-alkyl epoxides (e,g, methyloxirane) react with nucleophiles predominantly at the less hindered terminal carbon by a S_N2 mechanism, the situation with IP-1,2-O is more complex because of stereoelectronic effects from the ethenyl group, which may facilitate an internal S_N2 or S_N2-like pathway (53). The precise mechanistic details of the reactions described at the internal carbon of IP-1,2-O requires further study. The designation S_N2 in this paper should be taken primarily as a description of the established stereochemical outcome for the adducts characterized.

While exact quantification is not possible under the experimental conditions of the present study, comparing UV-peak heights of the respective regioisomers suggests a greater formation of N^6-dAdo adducts with the terminal oxirane carbon of either monoepoxide compared to the respective internal oxirane carbon. Since adducts on N^6-dAdo can theoretically originate either from Dimroth rearrangement of N1-dAdo adducts or via direct alkylation, in our study it was not possible to determine the reactivity of the internal or external oxirane carbons of the isoprene monoepoxides towards the N^6- (or N1-) position. Studies with epoxides containing substituents capable of delocalizing positive charge by conjugation, such as styrene oxide and butadiene monoepoxide, show that direct alkylation of the N^6-position of adenosine occurs mainly on the internal oxirane carbon, predominantly by a S_N1 mechanism (as reviewed in 36). In contrast, it was demonstrated that N^6- dAdo adducts on the terminal oxirane carbon of styrene oxide were exclusively formed by Dimroth rearrangement of N1-dAdo adducts (40;54).

Incubation of dAdo with pure *S*-IP-1,2-O and *S*-IP-3,4-O resulted in formation of predominant diastereomeric N^6-dAdo adducts from reactions at the internal oxirane carbon (**dAdo-2** and **dAdo-7**, respectively (Figure S22 and S23). As discussed above, this result does not support adduct formation via a S_N1 reaction but rather indicates that the adducts are mainly formed via S_N2 mechanism, with IP-3,4-O as well as with IP-1,2-O. Our study was not designed to enable us to make a distinction between N^6-dAdo adducts at the internal oxirane carbon of isoprene monoepoxides originating from Dimroth rearrangement of an N1-dAdo adduct or direct alkylation of N^6. It cannot be assumed that the proposed reaction mechanism and the results with butadiene monoepoxide and styrene oxide as described above are predictive of the origin of the detected isoprene monoepoxide N^6-dAdo adducts.

In contrast to the diastereomeric adducts formed from reaction at the internal oxirane carbon, the *R*- and *S*-diastereomers of adducts at the terminal oxirane carbon could not be chromatographically resolved for either of the isoprene monoepoxides.

Due to the small quantities of potential N1-dIno adducts detected after reaction of dAdo with IP-1,2-O, these were not further investigated. Reaction of IP-3,4-O at N1 of dAdo and subsequent deamination preferentially produced internal oxirane adducts judging by UV peak heights of the diastereomeric adduct pairs **dIno-2** and **-3** and **dIno-4** and **-5**. This observation is in accord with results of other investigators. Qian and Dipple (54) reported that deamination of N1-adenosine adducts on the terminal oxirane carbon of styrene oxide was very slow in comparison to deamination of adducts on the internal oxirane carbon. It was suggested that deamination occurs by a mechanism in which the hydroxyl group of the side-chain displaces the exocyclic (N^6) amino group intramolecularly to form an oxazolinium ring system. This reactive intermediate could then be opened by water, facilitating a nucleophilic attack at the C6- position of the purine. The observed higher deamination rate for the styrene oxide adduct on the internal oxirane carbon was thought to be due to the higher nucleophilicity of its hydroxyl-group relative to the hydroxyl-group in closer proximity to the phenyl ring (54). Preliminary results from reactions of isoprene monoepoxides with ssDNA suggest that the proportion of deaminated products (N1-hypoxanthine adducts) increased for adducts on the terminal oxirane carbon when dAdo was incorporated into DNA and implied that DNA structure favors this reaction (data not shown), which has been reported previously (40). In contrast to the deamination of N1-dAdo adducts (Figure 2a), direct reaction of N1-dIno with IP-3,4-O seemed to occur preferentially on the terminal oxirane carbon (Figure S1a). Our experiments were not designed to determine whether the differences in adduct yields are due to selective deamination of N1 adducts of dAdo adducts at the internal oxirane carbon, or to a difference in the reactivity of the oxirane carbons towards N1 of dAdo relative to N1 of dIno. Preferential reaction with the terminal oxirane carbon of IP-3,4-O with the endocyclic N1 nitrogen of dIno is in

contrast to our findings for the reaction of IP-3,4-O with N7 of dGua, where adducts were formed preferentially on the internal oxirane carbon (35). As observed above, it is also noteworthy that the adduct at the internal oxirane carbon of IP-3,4-O appears to form via a S_N2 substitution, in contrast to reports of an S_N1 substitution for butadiene monoepoxide and styrene oxide (36).

Although the N3 position of Ade has been reported to be a major alkylation site in DNA, steric hindrance due to intra- or intermolecular hydrogen-bonding of the N3-position is thought to hamper adduct formation at this position in the free nucleosides (36;55). Accordingly, N3-Ade adducts were not identified in the present study. It is likely that they were formed in insufficient amounts for collection and characterization. A product that eluted close to a peak suspected to be an N3-Ade adduct based on its UV spectrum was unequivocally identified as the N7-Ade adduct on the internal oxirane carbon of IP-3,4-O (**Ade-1**). Both **Ade-1** and the unidentified product, were detected in the chromatograms of the reaction mixture of IP-3,4-O with dAdo before and after hydrolysis.

N1-Deoxyinosine adducts have been shown to be highly mutagenic in site-directed mutagenesis studies. The mutagenicity is believed to reside in the structural similarity between inosine and guanosine. Inosine or its corresponding base, hypoxanthine, pair predominantly with cytosine and to a smaller extent with the other bases in the order I-C > I-A > I-G = I-T (56;57). Therefore, the presence of dIno, instead of dAdo in DNA, has the potential to lead to the incorporation of an incorrect base. Although an adduct on the N1-position could block Watson-Crick base pairing, N1-dIno adducts of butadiene epoxides have been demonstrated to be easily bypassed during replication and lead to mutations in *in vitro* experiments in *Escherichia coli* and mammalian cells, with A → G transitions being the predominant mutations (42;58). Additionally, as discussed above, the extent of the deamination reaction of N1-Ade adducts leading to these adducts is dependent on the specific adduct stereo- and regio-chemistry (54). The formation of N1-Ade or N1-Ado adducts has been well established *in vitro* (45;46). Furthermore, one study in workers exposed to butadiene detected N1-Ade adducts by ^{32}P-postlabeling (39). N1-hypoxanthine adducts were not detected *in vivo* in one study in mice and rats exposed to 625 ppm butadiene for 10 days (Boysen, unpublished results).

The mutational potential of N^6-Ade adducts seems to be rather low and largely dependent on the bulkiness of the adduct and its stereochemical conformation (59;60). However, these adducts could be used as stable biomarkers of internal exposure (36).

Similar to N3-dAdo or N7-dGuo adducts, N7 adducts of dAdo with IP-3,4-O readily deglycosylated, giving rise to abasic sites in DNA. Although abasic sites can be repaired and therefore might not have a high potential to lead to mutations, the base adducts might be used as biomarkers of exposure. For example, N7-Gua adducts can be detected in urine (51).

In conclusion, this is the first study to demonstrate formation of adducts of isoprene monoepoxides with dAdo. Both isoprene monoepoxides formed N^6-dAdo and/or N1-dIno adducts on the external as well as internal oxirane carbons. Furthermore, we identified an N7-Ade adduct at the internal oxirane carbon of IP-3,4-O. Describing the exact structure of adducts formed by isoprene monoepoxides with deoxynucleosides and subsequently those formed with DNA can serve as an initial step toward evaluating their potential for mutation or for use as biomarkers of isoprene metabolism and internal exposure.

Supplementary Material

Refer to Web version on PubMed Central for supplementary material.

Acknowledgments

FUNDING SUPPORT

This work was supported in part by grants from the International Institute of Synthetic Rubber Producers, Inc. and the NIH (P30-CA16086, P30-ES10126, and R42-ES11746).

Ms. Patricia Upton is thanked for her editorial assistance.

References

1. International Agency for Research on Cancer (IARC). IARC Monogr Eval Carcinog Risks Hum. Vol. 71. Lyon, France: 1999. Re-evaluation of some organic chemicals, hydrazine and hydrogen peroxide; p. 1015-1025.
2. International Agency for Research on Cancer (IARC). Overall Evaluations of Carcinogenicity to Humans. List of all agents, mixtures and exposures evaluated to date. Lyon, France: 2008. http://monographs.iarc.fr/ENG/Classification/crthall.php
3. National Toxicology Program (NTP). Eleventh Report on Carcinogens. Research Triangle Park, NC: 2005. 11th ROC: Isoprene.
4. World Health Organization (WHO). WHO Technical Report Series No. 951. Geneva, Switzerland: 2008. The Scientific Basis of Tobacco Product Regulation. Second Report of a WHO Study Group.
5. Graedel, TE.; Hawkins, DT.; Claxton, LD. Atmospheric Chemical Compounds. Sources, Occurrence, and Bioassay. Academic Press; Orlando, FL: 1986.
6. Elmenhorst H, Harke HP. Volatile components of tobacco smoke. Preparative yield of a gas-phase condensate. Z Naturforsch B. 1968; 23(9):1271–1272. [PubMed: 4387211]
7. Lofroth G, Stensman C, Brandhorst-Satzkorn M. Indoor sources of mutagenic aerosol particulate matter: smoking, cooking and incense burning. Mutat Res. 1991; 261 (1):21–28. [PubMed: 1881406]
8. Wallace LA, Pellizzari ED. Personal air exposures and breath concentrations of benzene and other volatile hydrocarbons for smokers and nonsmokers. Toxicol Lett. 1987; 35 (1):113–116. [PubMed: 3810671]
9. Leber AP. Overview of isoprene monomer and polyisoprene production processes. Chem Biol Interact. 2001:135–136. 169–173.
10. Lynch J. Occupational exposure to butadiene, isoprene and chloroprene. Chem Biol Interact. 2001:135–136. 207–214.
11. Sharkey TD. Isoprene synthesis by plants and animals. Endeavour. 1996; 20(2):74–78. [PubMed: 8690002]
12. Kuzma J, Nemecek-Marshall M, Pollock WH, Fall R. Bacteria produce the volatile hydrocarbon isoprene. Curr Microbiol. 1995; 30(2):97–103. [PubMed: 7765889]
13. Gelmont D, Stein RA, Mead JF. Isoprene-the main hydrocarbon in human breath. Biochem Biophys Res Commun. 1981; 99 (4):1456–1460. [PubMed: 7259787]
14. Barrefors G, Petersson G. Assessment of ambient volatile hydrocarbons from tobacco smoke and from vehicle emissions. J Chromatogr. 1993; 643(1–2):71–76. [PubMed: 7689578]
15. NTP. NTP Toxicology and Carcinogenesis Studies of Isoprene (CAS No. 78-79-5) in F344/N Rats (Inhalation Studies). Natl Toxicol Program Tech Rep Ser. 1999; 486:1–176. [PubMed: 12571689]
16. Placke ME, Griffis L, Bird M, Bus J, Persing RL, Cox LA Jr. Chronic inhalation oncogenicity study of isoprene in B6C3F1 mice. Toxicology. 1996; 113(1–3):253–262. [PubMed: 8901906]
17. Melnick RL, Sills RC, Roycroft JH, Chou BJ, Ragan HA, Miller RA. Isoprene, an endogenous hydrocarbon and industrial chemical, induces multiple organ neoplasia in rodents after 26 weeks of inhalation exposure. Cancer Res. 1994; 54 (20):5333–5339. [PubMed: 7923161]
18. Melnick RL, Sills RC, Roycroft JH, Chou BJ, Ragan HA, Miller RA. Inhalation toxicity and carcinogenicity of isoprene in rats and mice: comparisons with 1,3-butadiene. Toxicology. 1996; 113(1–3):247–252. [PubMed: 8901905]
19. Hong HL, Devereux TR, Melnick RL, Eldridge SR, Greenwell A, Haseman J, Boorman GA, Sills RC. Both K-ras and H-ras protooncogene mutations are associated with Harderian gland

tumorigenesis in B6C3F1 mice exposed to isoprene for 26 weeks. Carcinogenesis. 1997; 18(4): 783–789. [PubMed: 9111215]

20. Sills RC, Hong HL, Melnick RL, Boorman GA, Devereux TR. High frequency of codon 61 K-ras A-->T transversions in lung and Harderian gland neoplasms of B6C3F1 mice exposed to chloroprene (2-chloro-1,3-butadiene) for 2 years, and comparisons with the structurally related chemicals isoprene and 1,3-butadiene. Carcinogenesis. 1999; 20(4):657–662. [PubMed: 10223196]
21. Del Monte M, Citti L, Gervasi PG. Isoprene metabolism by liver microsomal mono-oxygenases. Xenobiotica. 1985; 15(7):591–597. [PubMed: 4049899]
22. Chiappe C, De Rubertis A, Tinagli V, Amato G, Gervasi PG. Stereochemical course of the biotransformation of isoprene monoepoxides and of the corresponding diols with liver microsomes from control and induced rats. Chem Res Toxicol. 2000; 13 (9):831–838. [PubMed: 10995255]
23. Bogaards JJ, Venekamp JC, van Bladeren PJ. The biotransformation of isoprene and the two isoprene monoepoxides by human cytochrome P450 enzymes, compared to mouse and rat liver microsomes. Chem Biol Interact. 1996; 102 (3):169–182. [PubMed: 9021169]
24. Bogaards JJ, Venekamp JC, Salmon FG, van Bladeren PJ. Conjugation of isoprene monoepoxides with glutathione, catalyzed by alpha, mu, pi and theta-class glutathione S-transferases of rat and man. Chem Biol Interact. 1999; 117 (1):1–14. [PubMed: 10190541]
25. Buckley LA, Coleman DP, Burgess JP, Thomas BF, Burka LT, Jeffcoat AR. Identification of urinary metabolites of isoprene in rats and comparison with mouse urinary metabolites. Drug Metab Dispos. 1999; 27(7):848–854. [PubMed: 10383931]
26. Vogelstein B, Kinzler KW. The multistep nature of cancer. Trends Genet. 1993; 9 (4):138–141. [PubMed: 8516849]
27. Swenberg JA, Richardson FC, Boucheron JA, Dyroff MC. Relationships between DNA adduct formation and carcinogenesis. Environ Health Perspect. 1985; 62:177–183. [PubMed: 4085420]
28. Farmer PB, Singh R. Use of DNA adducts to identify human health risk from exposure to hazardous environmental pollutants: the increasing role of mass spectrometry in assessing biologically effective doses of genotoxic carcinogens. Mutat Res. 2008; 659 (1–2):68–76. [PubMed: 18468947]
29. Gervasi PG, Citti L, Del Monte M, Longo V, Benetti D. Mutagenicity and chemical reactivity of epoxidic intermediates of the isoprene metabolism and other structurally related compounds. Mutat Res. 1985; 156 (1–2):77–82. [PubMed: 3158813]
30. Gervasi PG, Longo V. Metabolism and mutagenicity of isoprene. Environ Health Perspect. 1990; 86:85–87. [PubMed: 2401275]
31. Fabiani R, Rosignoli P, De BA, Fuccelli R, Morozzi G. DNA-damaging ability of isoprene and isoprene mono-epoxide (EPOX I) in human cells evaluated with the comet assay. Mutat Res. 2007; 629(1):7–13. [PubMed: 17317274]
32. Golding BT, Cottrell L, Mackay D, Zhang D, Watson WP. Stereochemical and kinetic comparisons of mono- and diepoxide formation in the in vitro metabolism of isoprene by liver microsomes from rats, mice, and humans. Chem Res Toxicol. 2003; 16 (7):933–944. [PubMed: 12870896]
33. Bleasdale C, Small RD, Watson WP, Wilson J, Golding BT. Studies on the molecular toxicology of buta-1,3-diene and isoprene epoxides. Toxicology. 1996; 113(1–3):290–293. [PubMed: 8901910]
34. Tareke E, Golding BT, Small RD, Tornqvist M. Haemoglobin adducts from isoprene and isoprene monoepoxides. Xenobiotica. 1998; 28(7):663–672. [PubMed: 9711810]
35. Begemann P, Christova-Georgieva NI, Sangaiah R, Koc H, Zhang D, Golding BT, Gold A, Swenberg JA. Synthesis, characterization, and identification of N7-guanine adducts of isoprene monoepoxides in vitro. Chem Res Toxicol. 2004; 17 (7):929–936. [PubMed: 15257618]
36. Koskinen M, Plna K. Specific DNA adducts induced by some mono-substituted epoxides in vitro and in vivo. Chem Biol Interact. 2000; 129(3):209–229. [PubMed: 11137062]
37. Tretyakova N, Sangaiah R, Yen TY, Gold A, Swenberg JA. Adenine adducts with diepoxybutane: isolation and analysis in exposed calf thymus DNA. Chem Res Toxicol. 1997; 10 (10):1171–1179. [PubMed: 9348440]

38. Selzer RR, Elfarra AA. In vitro reactions of butadiene monoxide with single- and double-stranded DNA: characterization and quantitation of several purine and pyrimidine adducts. Carcinogenesis. 1999; 20(2):285–292. [PubMed: 10069466]
39. Zhao C, Vodicka P, Sram1 RJ, Hemminki K. Human DNA adducts of 1,3-butadiene, an important environmental carcinogen. Carcinogenesis. 2000; 21(1):107–111. [PubMed: 10607741]
40. Barlow T, Takeshita J, Dipple A. Deamination and Dimroth rearrangement of deoxyadenosine-styrene oxide adducts in DNA. Chem Res Toxicol. 1998; 11 (7):838–845. [PubMed: 9671547]
41. Kowalczyk A, Harris CM, Harris TM. Synthesis and characterization of oligodeoxynucleotides containing an N1 beta-hydroxyalkyl adduct of 2′-deoxyinosine. Chem Res Toxicol. 2001; 14 (6): 746–753. [PubMed: 11409946]
42. Rodriguez DA, Kowalczyk A, Ward JB Jr, Harris CM, Harris TM, Lloyd RS. Point mutations induced by 1,2-epoxy-3-butene N1 deoxyinosine adducts. Environ Mol Mutagen. 2001; 38 (4): 292–296. [PubMed: 11774359]
43. Harwood LM, Casy G, Sherlock J. A simple laboratory procedure for preparation of (1-methylethenyl)oxirane (3,4-epoxyisoprene). Synth Commun. 1990; 20:1287–1292.
44. Singer, B.; Grunberger, D. Molecular Biology of Mutagenesis and Carcinogenesis. Plenum Press; New York: 1983.
45. Tretyakova N, Lin Y, Sangaiah R, Upton PB, Swenberg JA. Identification and quantitation of DNA adducts from calf thymus DNA exposed to 3,4-epoxy-1-butene. Carcinogenesis. 1997; 18 (1):137–147. [PubMed: 9054600]
46. Selzer RR, Elfarra AA. Characterization of N1- and N6-adenosine adducts and N1-inosine adducts formed by the reaction of butadiene monoxide with adenosine: evidence for the N1-adenosine adducts as major initial products. Chem Res Toxicol. 1996; 9 (5):875–881. [PubMed: 8828924]
47. Esmans EL, Broes D, Hoes I, Lemiere F, Vanhoutte K. Liquid-chromatography-mass spectrometry in nucleoside, nucleotide and modified nucleotide characterization. J Chromatogr A. 1998; 794:109–127.
48. Plavec J, Tong W. How Do the Gauche and Anomeric Effects Drive the Pseudorotational Equilibrium of the Pentofuranose Moiety of Nucleosides? J Am Chem Soc. 1993; 115:9734–9746.
49. Ippel JH, Wijrnenga SS, de Jong R, Heus HA, Hilbers CW, de Vroom E, van der Marel GA, van Boom JH. Heteronuclear Scalar Couplings in the Bases and Sugar Rings of Nucleic Acids: Their Determination and Application in Assignment and Conformational Analysis. Magnetic Resonance in Chemistry. 1996; 34:S156–Sl76.
50. Günther, HNMR. Spectroscopy. John Wiley and Sons; New York: 1995.
51. Boysen G, Pachkowski BF, Nakamura J, Swenberg JA. The formation and biological significance of N7-guanine adducts. Mutat Res. 2009; 678 (2):76–94. [PubMed: 19465146]
52. Watson WP, Cottrell L, Zhang D, Golding BT. Metabolism and molecular toxicology of isoprene. Chem Biol Interact. 2001:135–136. 223–238.
53. Ellis MK, Golding BT, Watson WP. Intrinsic reactivities in the alkylations of protected amino-acids by (R)-methyloxirane and (S)-methyloxirane. J Chem Soc Perkin Trans. 1984; 2:1737–1743.
54. Qian C, Dipple A. Different mechanisms of aralkylation of adenosine at the 1- and N6-positions. Chem Res Toxicol. 1995; 8 (3):389–395. [PubMed: 7578925]
55. Carrell HL, Glusker JP, Moschel RC, Hudgins WR, Dipple A. Crystal structure of a carcinogen:nucleoside adduct. Cancer Res. 1981; 41 (6):2230–2234. [PubMed: 6786734]
56. Martin FH, Castro MM, boul-ela F, Tinoco I Jr. Base pairing involving deoxyinosine: implications for probe design. Nucleic Acids Res. 1985; 13 (24):8927–8938. [PubMed: 4080553]
57. Case-Green SC, Southern EM. Studies on the base pairing properties of deoxyinosine by solid phase hybridisation to oligonucleotides. Nucleic Acids Res. 1994; 22(2):131–136. [PubMed: 8121796]
58. Kanuri M, Nechev LV, Tamura PJ, Harris CM, Harris TM, Lloyd RS. Mutagenic spectrum of butadiene-derived N1-deoxyinosine adducts and N6, N6-deoxyadenosine intrastrand cross-links in mammalian cells. Chem Res Toxicol. 2002; 15 (12):1572–1580. [PubMed: 12482239]
59. Carmical JR, Nechev LV, Harris CM, Harris TM, Lloyd RS. Mutagenic potential of adenine N(6) adducts of monoepoxide and diolepoxide derivatives of butadiene. Environ Mol Mutagen. 2000; 35(1):48–56. [PubMed: 10692227]

60. Scholdberg TA, Nechev LV, Merritt WK, Harris TM, Harris CM, Lloyd RS, Stone MP. Mispairing of a site specific major groove (2S,3S)-N6-(2,3,4-trihydroxybutyl)-2′-deoxyadenosyl DNA Adduct of butadiene diol epoxide with deoxyguanosine: formation of a dA(anti). dG(anti) pairing interaction. Chem Res Toxicol. 2005; 18 (2):145–153. [PubMed: 15720118]

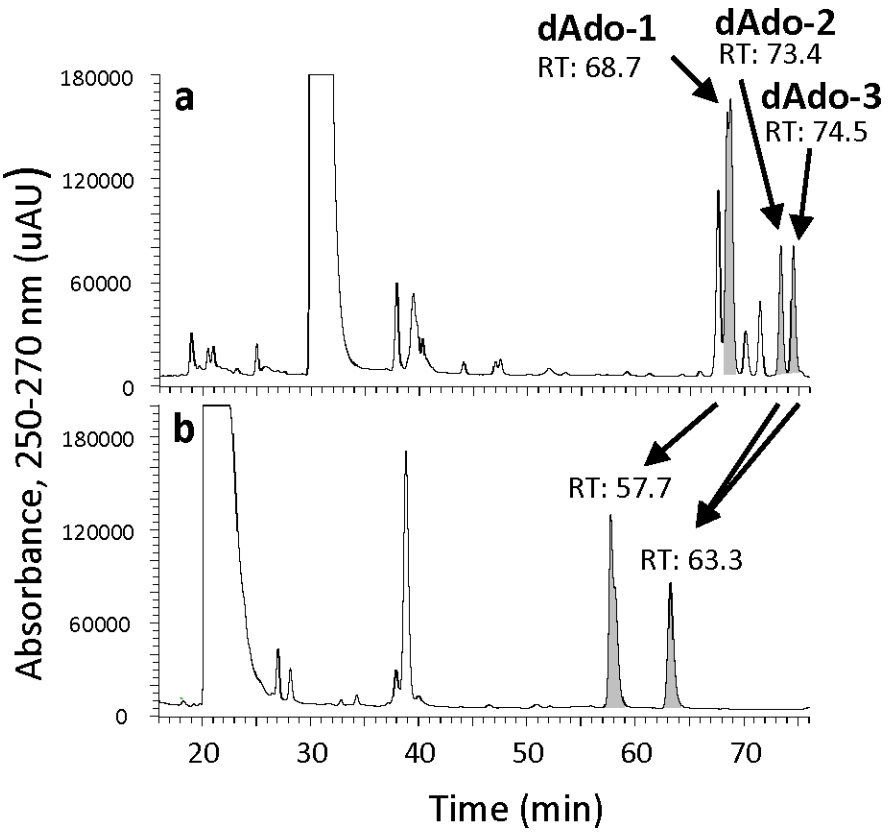

Figure 1.
HPLC/DAD analysis of the reaction mixtures of IP-1,2-O with dAdo before (a) and after mild acid hydrolysis (b). Separation on a 4.6 × 250 mm C18 Aquasil column, 1 mL/min, gradient program 1.

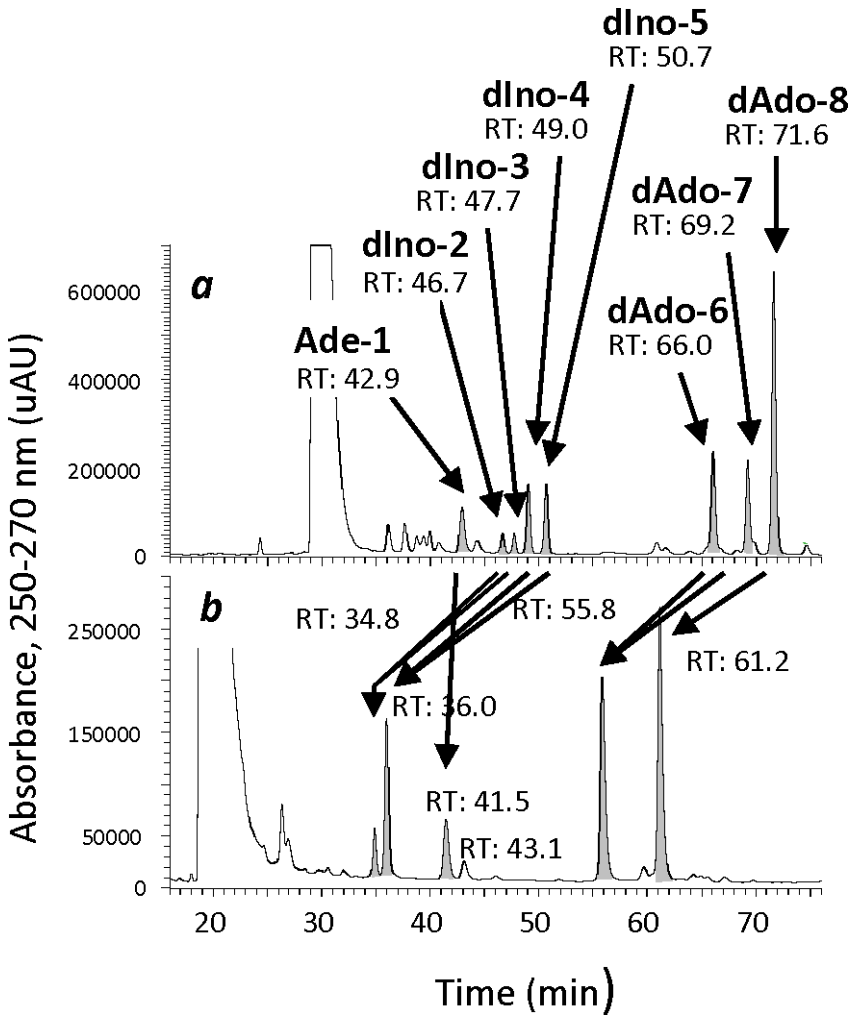

Figure 2.

HPLC/DAD analysis of the reaction mixtures of IP-3,4-O with dAdo before (a) and after mild acid hydrolysis (b). Separation on a 4.6 × 250 mm C18 Aquasil column, 1 mL/min, gradient program 1.

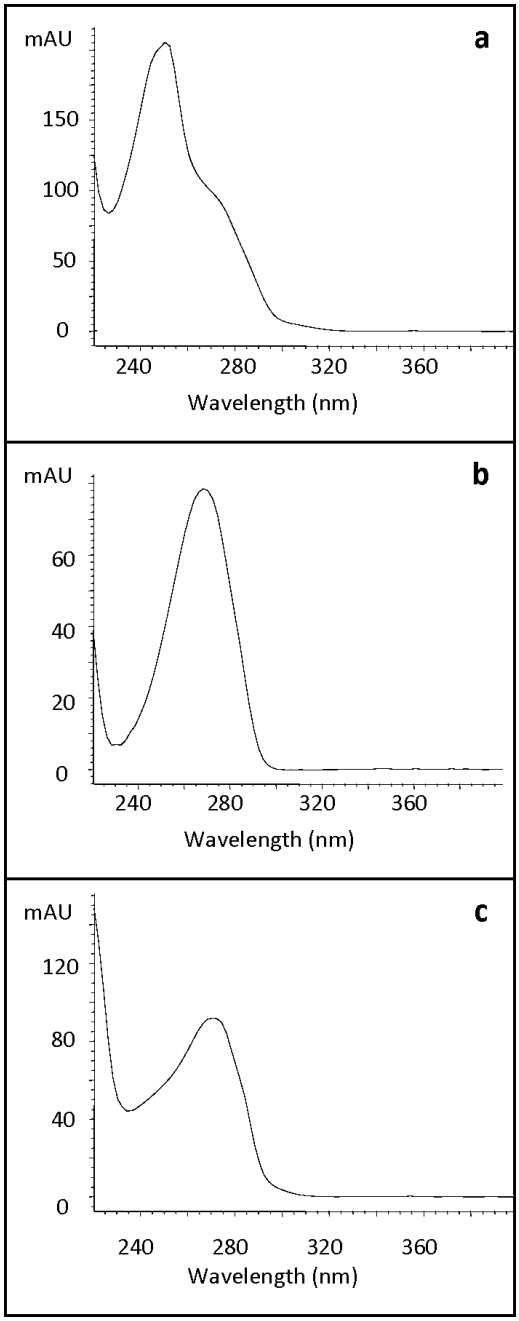

Figure 3.
Representative UV-Spectra for (a) N1-dIno adducts, (b) N^6-dAde adducts, and (c) N7-Ade adducts.

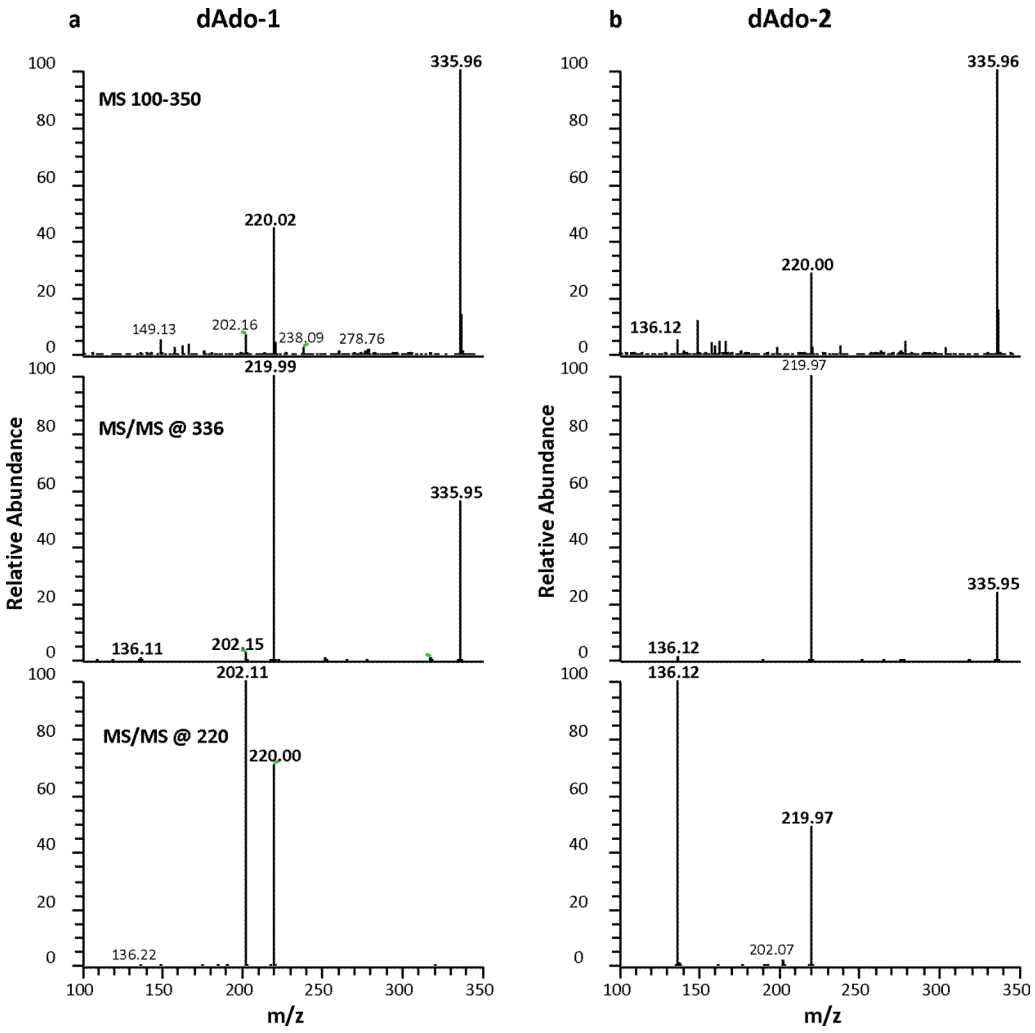

Figure 4.

Representative MS spectra for terminal (C1) and internal (C2) N^6-dAdo adducts derived from reaction with IP-1,2-O. Shown are the full scan m/z 100 to 400 (top spectrum), the product ion spectrum from ions m/z 336 (middle) and m/z 220 (bottom) of **dAdo-1** (A) and **dAdo-2** (B), respectively.

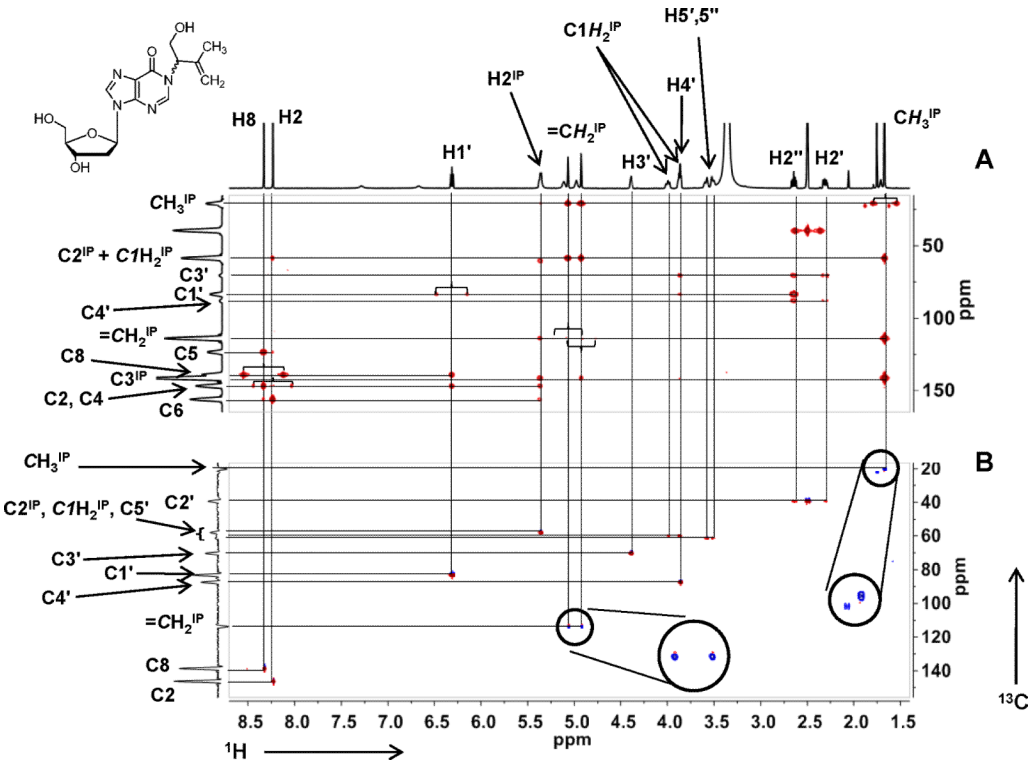

Figure 5.

HMBC (A) and HSQC (B) spectra of the N1-dIno adduct of IP-3,4-O at the internal oxirane carbon (**dIno-5**). Carbon and proton signal assignments are indicated on the marginal traces. In the HMBC spectrum, unsuppressed 1-bond couplings are indicated by brackets. Key features of the HMBC spectrum in establishing regiochemistry of addition are cross peaks between $H2^{IP}$ of the isoprene side-chain and C2 and C6 of the purine nucleus and the 2 ppm difference (not resolved) in chemical shifts between $C1^{IP}$ and $C2^{IP}$. C,H connectivities are indicated by solid lines. In the HSQC spectrum the C,H couplings of the isoprene vinyl protons and methyl protons CH_3^{IP} (blue) are negatively phased.

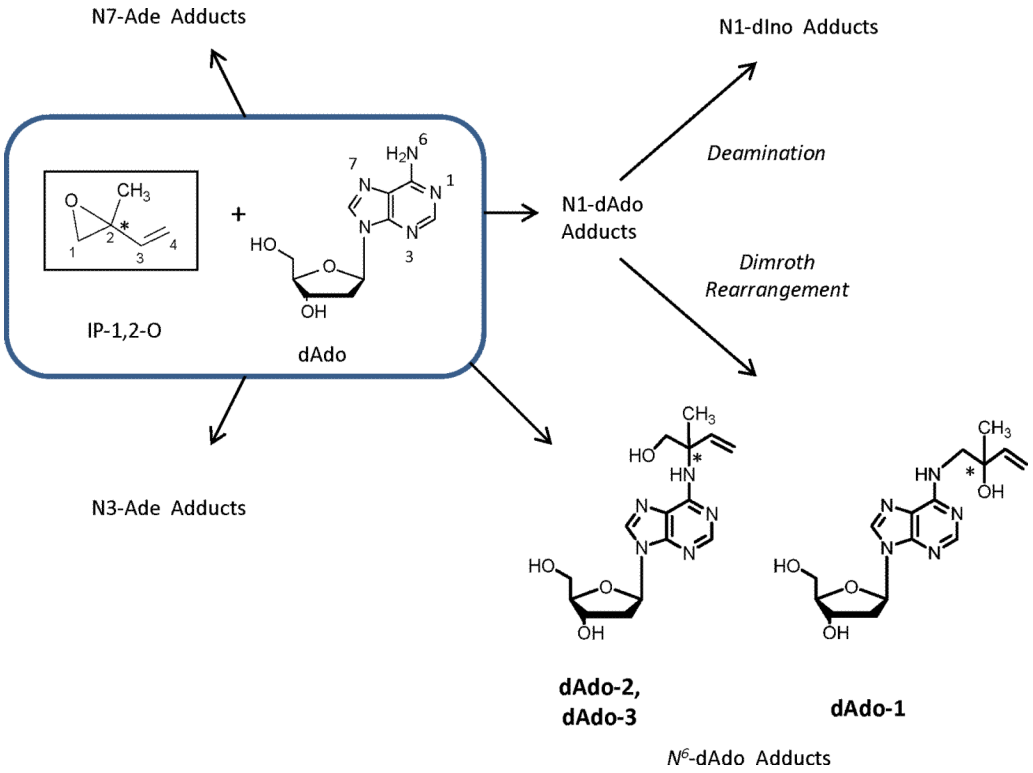

Scheme 1.
Proposed Adduct Formation of Isoprene Monoepoxides on dAdo: Example IP-1,2-O. * Indicates a chiral center.

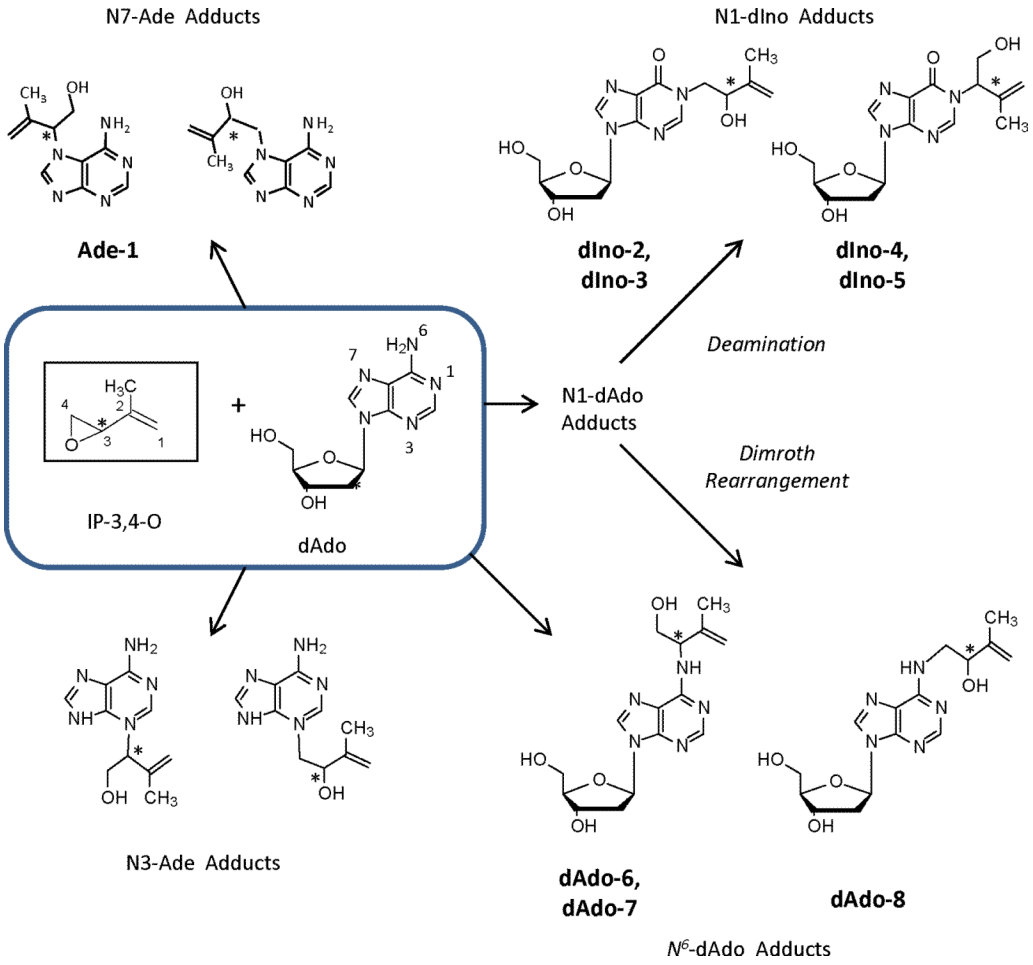

Scheme 2.
Proposed Adduct Formation of Isoprene Monoepoxides on dAdo: Example IP-3,4-O. * Indicates a chiral center.

Table 1

Products identified after reaction of isoprene monoepoxides (IP-1,2-O and IP-3,4-O, respectively) with 2′-deoxyadenosine (dAdo) *in vitro* (50 mM phosphate buffer, pH 7.4, 37ºC).

dAdo Reaction with	Product Name	Product Identification(Corresponding to IP-1,2-O and IP-3,4-O)	Product Name According to IUPAC Nomenclature	MW	Retention Time (min) Analytical (Semi-preparative)	Main Fragments (m/z) Full ms^2 of m/z 220 or 221, respectively	UV λ_{max} (nm)
IP-1,2-O	dAdo-1*	*R,S*-C1-N^6-dAdo	N^6-(1-(2R,*S*-2-hydroxy-2-methylbut-3-enyl)-2′-deoxyadenosine	335	(73.9)	202 > 220	270
				335	68.7		265
	dAdo-2*	*R*-C2-N^6-dAdo	N^6-(2-(2*R*-1-hydroxy-2-methylbut-3-enyl)-2′-deoxyadenosine	335	73.4 (78.0)	136 > 220	270
	dAdo-3	*S*-C2-N^6-dAdo	N^6-(2-(2*S*-1-hydroxy-2-methylbut-3-enyl)-2′-deoxyadenosine	335	74.5 (79.4)	136 > 220	270
IP-3,4-O	dAdo-6	*S*-C3-N^6-dAdo	N^6-(2-(2*S*-1-hydroxy-3-methylbut-3-enyl)-2′-deoxyadenosine	335	66.0 (71.4)	220 ≫ 202 ≈ 136	270
	dAdo-7	*R*-C3-N^6-dAdo	N^6-(2-(2*R*-1-hydroxy-3-methylbut-3-enyl)-2′-deoxyadenosine	335	69.2 (74.5)	220 ≫ 202 ≈ 136	270
	dAdo-8*	*R,S*-C4-N^6-dAdo	N^6-(1-(2R,*S*-2-hydroxy-3-methylbut-3-enyl)-2′-deoxyadenosine	335	71.6 (76.9)	220 > 202 > 148 > 136	265
				335			
	dIno-2*	*S*-C4-*N1*-dIno	*N*1-(1-(2*S*-2-hydroxy-3-methylbut-3-enyl)-2′-deoxyinosine	336	46.7 (52.4)	221 > 203 > 139 ≈137	250
	dIno-3	*R*-C4-*N1*-dIno	*N*1-(1-(2*R*-2-hydroxy-3-methylbut-3-enyl)-2′-deoxyinosine	336	47.7	221 > 203 > 139 ≈ 137	250
	dIno-4	*R*-C3-*N1*-dIno	*N*1-(2-(2*R*-1-hydroxy-3-methylbut-3-enyl)-2′-deoxyinosine	336	49.0	137 > 221 > 203	250
	dIno-5*	*S*-C3- *N1*-dIno	*N*1-(2-(2*S*-1-hydroxy-3-methylbut-3-enyl)-2′-deoxyinosine	336	50.7 (56.4)	137 > 221 > 203	250
	Ade-1	*C3-N7-Ade*	*N7-(2-(1-hydroxy-3-methylbut-3-enyl)-2′-deoxyadenosine*	219	42.9 (50.3)	220 ≫ 136	270

* Indicates that accurate mass of the purified adduct has been determined and was >0.5 ppm of the theoretical mass (Table S1).